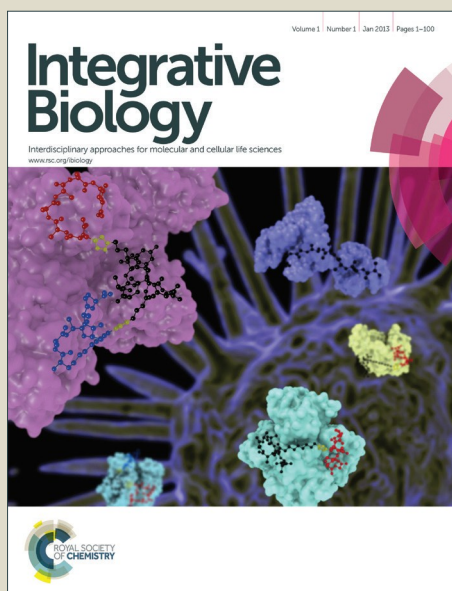


Integrative Biology

Accepted Manuscript



This is an *Accepted Manuscript*, which has been through the Royal Society of Chemistry peer review process and has been accepted for publication.

Accepted Manuscripts are published online shortly after acceptance, before technical editing, formatting and proof reading. Using this free service, authors can make their results available to the community, in citable form, before we publish the edited article. We will replace this *Accepted Manuscript* with the edited and formatted *Advance Article* as soon as it is available.

You can find more information about *Accepted Manuscripts* in the [Information for Authors](#).

Please note that technical editing may introduce minor changes to the text and/or graphics, which may alter content. The journal's standard [Terms & Conditions](#) and the [Ethical guidelines](#) still apply. In no event shall the Royal Society of Chemistry be held responsible for any errors or omissions in this *Accepted Manuscript* or any consequences arising from the use of any information it contains.

This paper provides new, detailed information on the morphological and migratory responses of human bone marrow-derived mesenchymal stem cells (hBM-MSCs) when stimulated with a wide range of electric field (EF) intensities, covering both physiological and aphysiological field strengths, for up to 15 hours of study. To enhance throughput and experimental reproducibility, a novel medium-throughput micro-device platform that allowed for up to 6 biological repeats to be performed at any one time was developed and validated. Using this new device platform, we show that hBM-MSCs migrate towards the cathode at EFs as low as 0.2V/cm, and that the speed of directed migration was dependent upon the applied EF strength. hBM-MSCs adopt an increasingly elongated shape and increasingly aligned perpendicularly to the field vector over a range of EF strengths varying from 0.2V/cm to 3 V/cm, and the development of actin fibres and focal adhesions (which are again perpendicular to the applied EF) is significantly perturbed in the presence of an EF. Lastly, we compared hBM-MSCs from 3 different donors, and show that individual variations in responses were found confirming that electrical stimulation of cells should be ideally tailored to the individual. Given its clear impact on cellular behaviours important to tissue engineering applications, imposing EFs in a controlled manner may prove to be a useful tool, particularly in the colonisation of scaffolds with potentially therapeutic MSCs in a directed and controlled manner, whilst ensuring cellular viability is maintained.

ARTICLE

Cite this: DOI:
10.1039/x0xx00000x

Effects of electric fields on human mesenchymal stem cell behaviour and morphology using a novel multichannel device

T.A. Banks^{1,2}, P. S. B. Luckman³, J. E. Frith¹, and J. J. Cooper-White^{1,4,5,*}

Received 00th January 2012,
Accepted 00th January 2012

DOI: 10.1039/x0xx00000x

www.rsc.org/

The intrinsic piezoelectric nature of collagenous-rich tissues, such as bone and cartilage, can result in the production of small, endogenous electric fields (EFs) during applied mechanical stresses. *In vivo*, these EFs may influence cell migration, a vital component of wound healing. As a result, the application of small *external* EFs to bone fractures and cutaneous wounds is actively practiced clinically. Due to the significant regenerative potential of stem cells in bone and cartilage healing, and their potential role in the observed improved healing *in vivo* post applied EFs, using a novel medium throughput device, we investigated the impacts of physiological and aphysiological EFs on human bone marrow-derived mesenchymal stem cells (hBM-MSCs) for up to 15 hours. The applied EFs had significant impacts on hBM-MSC morphology and migration; cells displayed varying degrees of conversion to a highly elongated phenotype dependent on the EF strength, consistent perpendicular alignment to the EF vector, and definitive cathodal migration in response to EF strengths ≥ 0.5 V/cm, with the fastest migration speeds observed at between 1.7 and 3V/cm. We observed variability in hBM-MSC donor-to-donor responses and overall tolerances to applied EFs. This study thus confirms hBM-MSCs are responsive to applied EFs, and their rate of migration towards the cathode is controllable depending on the EF strength, providing new insight into the physiology of hBM-MSCs and possibly a significant opportunity for the utilisation of EFs in directed scaffold colonisation *in vitro* for tissue engineering applications or *in vivo* post implantation.

Introduction

Physiologic processes as fundamental as the cell cycle, cell proliferation, establishment of left-right body asymmetry, embryonic cell migration, axon outgrowth, spinal cord repair, epithelial tissue repair, tissue regeneration, angiogenesis and matrix secretion have all been shown to be influenced by endogenous electric fields (EFs)¹. In terms of musculoskeletal tissues, EFs have also been detected during loading of articular cartilage explants², while piezoelectrically generated EFs have been detected in dry bone³, and streaming potentials are thought to be the mechanism for strain-generated potentials in wet bone⁴. The clinical use of exogenous EFs to treat healing musculoskeletal tissues *in vivo*, is on-going, particularly with the electrical stimulation of bone healing⁵, ligament healing⁶, articular cartilage repair⁷, and to delay the progression of osteoarthritis⁸. Additionally, humans with cervical osteoarthritis showed reduced pain, disability and muscle spasm, and increased range of motion⁹, and humans with knee osteoarthritis show improved physical function¹⁰, when treated with external EF therapy. *Ex vivo*, defects

in meniscus explants (bovine) showed increased strength of repair tissue when subjected to EFs in culture conditions for 6 weeks, with upwards trends in deoxyribonucleic acid (DNA) and hydroxyproline content (a major component of collagen)¹¹. It is only since the mid-1980s, however, that researchers have reported that cells in culture also migrate within a small, physiologic electric field (EF), a phenomenon termed electrotaxis or galvanotaxis¹². Galvanotaxis differs from galvanotropism (turning response or growth towards or away from an EF), in that the organism has motility and demonstrates guided movement towards or away from the EF. *In vitro*, EFs in the range of 0.1 to 10 V/cm are typically applied to produce electrotaxis¹⁰. Cellular electrotaxis in the presence of exogenously applied direct current (dc) EFs has also been observed to be highly directional, suggested to be due to activation of intracellular pathways in a polarised manner¹³, however migration rates of different cell types have been shown to vary significantly and not all cells migrate in the same direction¹⁴. Electrotactic cellular responses are thus expected to be cell-type, species, and stimulation parameter dependent^{13,14b}. For example, *in vitro* studies

have shown cathodal migration for osteoblasts, with cathodally-oriented lamellopodia and cellular elongation with their long axes perpendicular to the direction of movement^{12d}, whilst osteoclasts migrated towards the anode and displayed anodally-oriented lamellopodia and a fan-shaped morphology^{12d}. Chondrocytes stimulated with EFs *in vitro* elongated perpendicular to the EF vector and migrated cathodally with extension of lamellopodia at their leading edge¹⁵. Intriguingly, some whole cells will even migrate in the opposite direction to their own cell fragments¹⁶. *In vitro* studies to cells in culture have shown that applied EFs also influence not only migration (including cancer cell migration), but also cell proliferation, angiogenesis, and nerve growth and wound healing¹⁷. The exact mechanism/s by which cells respond to an EF remain to be well defined, although lateral electrophoresis, redistribution^{16, 18}, and mechanical torque¹⁹ on charged membrane proteins is believed to be involved. Additionally, electrostatic cues have been shown to induce polarization of PI3 kinase (phosphatidylinositol-3-OH kinase- γ) and Src (cellular sarcoma gene family kinases) pathways to the leading edge of migratory cells^{16, 20}, and a rho-associated protein kinase (ROCK)-dependent pathway to the rear edge^{16, 18b}. Polarization of the Golgi apparatus towards the cathodal side of the cell has also been documented in Chinese Hamster Ovary (CHO) cells migrating cathodally^{20b}.

With EFs inducing such perturbations of critical cellular pathways, it is of no surprise that EF-induced directedness of cell migration *in vitro* has been shown to override other coexisting physiological cues such as initial injury stimulation, gradients of chemoattractants, wound void, contact inhibition release, population pressure, and changes in mechanical force after injury^{20a, 21}. Further, evidence would suggest that the responsiveness of cells to an exogenously applied dc EF affects cells through the same or similar mechanisms as endogenous EFs^{1k, 13}. These observations have direct impact on the possibility of utilising EFs in a tissue engineering framework. Adult mesenchymal stem or stromal cells (MSCs) can be found in almost every type of tissue and are known to play vital roles in tissue regeneration and repair. They are seen as an ideal source of cells for tissue engineering and regenerative medicine applications due to their ability to self-renew and multilineage differentiation potentials²², especially into bone, cartilage and muscle. For the purposes of osteochondral tissue engineering, human bone marrow-derived mesenchymal stem cells (hBM-MSCs) are a common source of cells used in tissue engineering, and like human adipose-derived MSCs (hA-MSCs), have the advantage of being an autogenous cell

source. Compared to other sources of hMSCs, higher yields of MSCs are derived from BM compared to adipose tissue, Wharton's jelly or umbilical cord blood²³. Several studies have already shown their effective clinical for the treatment of bone defects²⁴, and cartilage defects²⁵.

Whilst the importance of *in vitro* continuous dc EF stimulation on other types of stem cells (induced pluripotent stem cells (hiPS cells), embryonic stem cells (hES), and neural stem cells derived from hES (hNSCs) has been studied²⁶, to date the only human MSCs investigated in this way are hBM-MSCs²⁷ and hA-MSCs²⁸. Tandon et al. (2009) reported hA-MSCs disassembled gap junctions, aligned actin stress fibres, elongated and aligned perpendicular to the applied EF vector²⁸. Interestingly, mouse A-MSCs showed an increase in cathodal directedness values as well as cellular orientation perpendicular to the EF vector, and migration speeds as EF strength increased from 1, 6 and 10 V/cm²⁹. In the first study of investigations into the effects of EFs on hBM-MSCs²⁷, the authors found that hBM-MSCs from 3 donors migrated towards the anode, and that this directional migration occurred at a threshold of between 1 and 2.5 V/cm, and was maintained for up to 8 hours under a 2 V/cm EF. In this study, migration speeds reached a peak at 3 V/cm EF stimulation. This key study also showed there was no reduction in cell viability after 2 hours of either 2 V/cm or 6 V/cm EF application. Additionally, hBM-MSCs of late passage (P7-P10) showed a reduction in the degree of directedness under EF stimulation when compared to early passage cells (P3-P5). The application of EFs to MSCs may have significant potential beyond electrotaxis alone, given that there have been reports of the application of EFs to bone cells in culture increasing osteoinductive bone morphogenic proteins³⁰ and TGF- β 1³¹, and chondrocytes in culture conditions stimulated with EFs produced more matrix proteins and proteoglycans³² and showed increased or decreased proliferative capacity depending on the EF strength³³. Human BM-MSCs seeded into 3-dimensional polycaprolactone scaffolds containing a sulphated hyaluronan derivative and stimulated with pulsed dc EFs showed increased osteogenic differentiation³⁴. Increased osteogenic differentiation was also seen with hBM-MSCs subjected to pulsed electromagnetic fields³⁵, and alternating current EFs³⁶. Low-frequency alternating EFs have also been applied to human A-MSCs *in vitro*, in which they displayed increased calcium signalling and deposition of calcium when cultured in osteogenic medium³⁷. High frequency pulsed dc EFs have also been applied to 3D micromass culture systems of human A-MSCs in conjunction

with TGF β 3 to induce chondrogenesis³⁸. Pulsed dc EFs have also been applied to mouse A-MSCs³⁹, and alternating EFs to murine neural stem cells^{40,41}. Previous reports of the influence of EFs on hBM-MSCs²⁷ have unfortunately only investigated a restricted range of dc EF strengths and duration of EF application, and the morphological cellular changes induced by the EFs were not reported. Further investigation into the responses of hBM-MSCs to applied EFs covering both physiological and aphysiological ranges of EFs for longer time points is highly likely to yield new insight into their physiology and the possibility of using EFs as a tool in regenerative medicine applications. In particular, we believe that the combination of multipotent stem cells, scaffolds and external EF stimulation shows considerable promise for future tissue engineering therapeutic strategies. We thus report here the outcomes of a detailed and systematic investigation into the morphological and migratory responses of STRO-1, VCAM-1 (vascular cell adhesion molecule 1)/ CD106 (cluster of differentiation 106) selected hBM-MSCs⁴², a unique primary cell source (so called mesenchymal precursor cells) with minimal batch variation, to a larger range of physiological and aphysiological dc EF stimulations of various magnitudes and durations than previously probed, using a novel, multi-channel cell migration device platform.

Materials and Methods

Cell Culture and Device for Electrotaxis

Passage 5 or 6 human BM-MSCs from primary cultures (provided by Mesoblast Ltd. as a gift) were expanded with media changes every 4 days until 80% confluent. Human BM-MSCs from three independent donors were assessed in this study, labelled A, B, C. Cells were then detached by 0.25% trypsin-EDTA (Invitrogen), neutralised with 10% foetal bovine serum (FBS; Invitrogen), centrifuged and seeded as passage 6 or 7 cells into 6 channel ibidi $\text{\textcircled{c}}$ ibiTreat μ -Slide VI (catalogue # IBI80606) cell culture devices at 20,000 cells per 100 μ L or 10,000 cells/ cm². These 6 channel ibidi $\text{\textcircled{c}}$ cell culture devices were modified to allow EF delivery to each of 6 cell culture chambers in parallel. It has been shown that incompletely spread cells will migrate more rapidly than fully spread cells⁴³, and so to ensure cell attachment was as uniform as possible for each experiment, hBM-MSCs were inoculated within the device, incubated at 37 $^{\circ}$ C, 95% relative humidity and 5% CO₂, overnight prior to EF exposure. Further, cell seeding density was kept consistent for all experiments, as cells in contact with each other will experience the voltage drop across their combined dimensions, by

communicating via gap junctions²⁸. Seeding density has been shown to influence cellular responses; as monolayers of 3T3 cells respond more sensitively than sparse cell populations *in vitro*⁴³, and tightly connected hiPS cell colonies migrate more slowly (2.4 ± 0.6 μ m/hr) but with greater anodal directionality compared to dissociated cells (30 ± 1.2 μ m/hr) *in vitro*^{26a}. Single cells also reorient themselves in response to the EF more quickly than cells in a monolayer sheet⁴⁴. Huang et al (2013) showed that 3T3 fibroblasts confined within a 20 μ m wide channel orient parallel to the EF vector and migrate faster than cells in 100 μ m wide channels, where cell alignment was perpendicular to the EF vector⁴⁵. The ibidi $\text{\textcircled{c}}$ microdevice used in this study had consistent channel dimensions (3.8 mm width x 17 mm length x 0.4 mm height), therefore avoiding any influence of a confined geometry on cellular alignment and migration speed.

Direct current EF stimulation

The 6 channel ibidi $\text{\textcircled{c}}$ device was placed on an automated microscope stage within a temperature controlled chamber (37 $^{\circ}$ C) with CO₂ delivered at 5 vol. %. The ibidi $\text{\textcircled{c}}$ device was customised to create an EF delivery system to allow up to 6 cell migration chambers to be stimulated simultaneously; where up to 6 pairs of salt bridges of 4% agarose in physiologic buffered saline (PBS) connected cell migration channels to reservoirs of PBS, in which Ag-AgCl electrodes were immersed (figure 1). Electrodes were then connected to an external current supply (Glassman FC Series PS/FC50-PO2, Glassman High Voltage, Inc., High Bridge, NJ) to deliver 0.1 to 2.4mA to achieve a dc EF of 0.2-5V/cm depending on whether 1, 2, 3 or 4 experimental channels were used. A voltmeter was used to measure the EF strength (E) in V/cm in the media reservoirs at either end of the cell migration channels. If only a single channel was used, the current delivered was 0.8, 0.5, 0.35, 0.25, 0.15, 0.05 or 0.03mA for EF strengths of 5, 3, 2, 1.7, 1.2, 0.5, or 0.2 V/cm respectively, corresponding to J values of approximately 0.053, 0.033, 0.023, 0.016, 0.01, 0.003, and 0.002 A/cm² respectively. The mean resistances (R) for experimental configurations of 1 to 4 experimental channels of the ibidi $\text{\textcircled{c}}$ ibiTreat μ -Slide VI cell culture device were calculated as 9.8, 8.5, 3.6 and 2.7 k Ω respectively using Ohm's law ($V = IR$).

Electro-osmotic fluid flow

The possible electro-osmotic flow (EOF) rate produced within a single channel of the 6 channel ibidi $\text{\textcircled{c}}$ device over the range of applied EFs is very difficult to estimate. Without actual measurement of the permittivity of our cell culture media (different to previously published medias that have measured the relative

permittivity⁴⁶), and the actual zeta potential of the surfaces within the ibidi® μ -slide flow chambers, which are a commercial product of undisclosed material composition, any theoretical calculation of the electro-osmotic mobility (U_{eo}) could be substantially incorrect. The base substrate within the ibidi® μ -slide flow chambers are also gas (and hence ion) permeable and have been modified to permit cell attachment (through the introduction of charges, both positive and negative). The zeta potential of a porous charged membrane is generally significantly lower than a solid surface made of the same material⁴⁷. We thus acknowledge that even in the absence of cells, this substrate will thus have a very different zeta potential to that of a solid glass or polystyrene substrate most commonly used in microfluidic devices using cell culture media and hence a very different U_{eo} , for example, to that calculated for cell culture media within a microfluidic device constructed of PDMS with a glass base of $1.34 \times 10^{-8} \text{ m}^2/(\text{Vs})$ ⁴⁸. Further, during experiments, the base of the device is covered with cells, which themselves will contribute to the charge balance. The actual zeta potential of the cell-coated ibidi® μ -slide flow chamber surface is thus very difficult to predict theoretically, and to even measure. In any case, the presence of cells within and beyond the boundary layer of any fluid flow will substantially disturb the flow, and we should thus even question the validity of using standard equations to predict the EOF in our complex scenario, which will likely substantially over predict any EOF present. In the absence of a reliable estimate of any EOF, but to demonstrate that any present flow is unlikely to be responsible for the observed directional migration response or the morphologic cellular changes observed with electric field stimulation, we performed pressure-driven fluid flow studies once for human BM-MSCs (donor D cells) exposed to either 6 or 20 $\mu\text{L}/\text{hour}$ continuous fluid flow or static conditions (control) for up to 8 hours.

Joule heating

The expected temperature after 15 hours of 0.8mA current application to a single chamber (to achieve a 5V/cm EF) was calculated to be 37.004 to 37.006°C (see supplementary materials). Additionally, the temperatures of cell migration chambers under EF or control (no EF) were measured. Comparisons of directional response, distances and speeds travelled were also compared for cells subjected to 43°C without an EF, and cells subjected to 38°C in conjunction with a 5 V/cm EF, and cell subjected to 37°C in conjunction with a 5 V/cm EF (see supplementary materials).

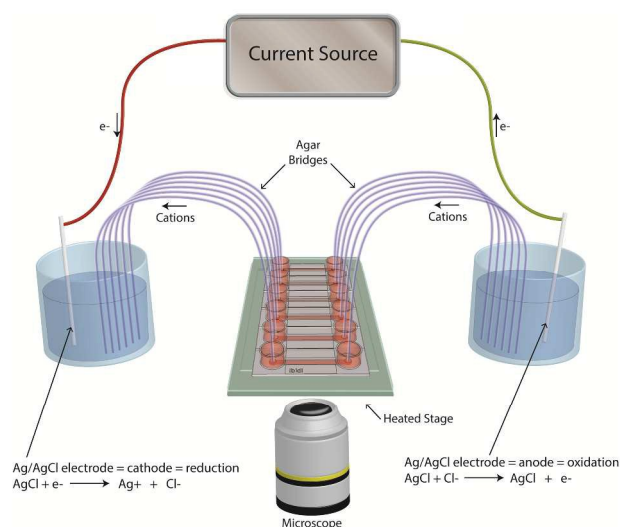


Fig 1. Schematic representation of experimental design

Measurement of cell migration

Time-lapse phase-contrast images were collected every 15 minutes over 15 hours for cells exposed to 0.2 V/cm, 0.5 V/cm, 1.2V/cm, 1.7 V/cm, 2V/cm, 3V/cm, 5V/cm, and no EF (control) using a real-time inverted microscope (Olympus IX81) connected to a computer and software (Cell-R, Olympus). Images were also taken every 15 minutes for donor A cells exposed to a 1.2V/cm EF for 4 hours, after which the direction of the EF was reversed, and images were again taken every 15 minutes for a further 4 hours. Additionally, images were taken every 15 minutes for donor D cells exposed to a 6 or 20 $\mu\text{L}/\text{hour}$ fluid flow, or no fluid flow (control) for up to 8 hours. All images were taken using x10 objective. MEM alpha medium (Gibco®) containing 10% foetal bovine serum (FBS), 0.5% sodium pyruvate (100x), 0.1% of 50mM ascorbic acid-2-phosphate (A2P) and 1% penicillin-streptomycin solution (Gibco®) (standard MSC culture media) was used for cell culture and EF exposure or fluid flow experiments. Experiments were performed in triplicate, each time using an independent culture population of passage 6 or 7 human MSCs from a single donor (donor A). Additionally, each experiment was performed once using passage 6 or 7 MSCs from 2 other donors (B and C) at the same EF strengths, and in triplicate for control studies.

Time-lapse image analysis

Time-lapse images were analysed using the ImageJ manual cell tracking tool (Version 1.45, NIH, Bethesda, MD) and chemotaxis tool (ibidi®) software for a minimum of 60 cells for control (no EF) and for each EF strength for donor A cells. This was repeated for a minimum of 20 cells for control (no EF) and experimental cells at

each EF strength for donor B and C cells, and a minimum of 20 cells for Donor D cells for control (static culture) and experimental (6 or 20 $\mu\text{L}/\text{hour}$ fluid flow) conditions. Cell tracking ceased if cells were seen to divide or leave the field of view. The cell nucleus determined the position of the cell in each frame. The displacement of individual cells and the elapsed time between successive image frames and cell number were used to determine a mean \pm SEM value for accumulated distance, euclidean distance and speed of migration. The direction of cell migration for each cell was extracted from plot charts to determine the percentage of cells migrating upwards (towards the cathode) (see supplementary materials tables S1-3). The ImageJ particle analyser tool was then used to determine a mean \pm SEM value for cell area (μm^2), fit ellipse circularity, aspect ratio, and fit ellipse angle for a minimum of twenty donor A cells at each EF strength at 0, 5, 10 and 15 hour time-points. The particle analyser tool was also used to obtain these values for donor D cells before and after fluid perfusion, or static culture (control). An ellipse is fitted to an outline of the cell, and circularity was determined using the formula $\text{circularity} = 4\pi \times \frac{[\text{area}]}{[\text{perimeter}]^2}$ with a value of 1.0 indicating a perfect circle, and a value approaching 0.0 indicating an increasingly elongated shape. To determine the fit ellipse angle, the angle between the primary axis of the ellipse and a line parallel to the x-axis was measured. The smallest angle from the x-axis was used (measured in a clockwise or anti-clockwise direction). The fit ellipse angle was divided by 90 to result in an orientation index. A cell with an orientation index of 1 would have its long axis aligned parallel to the EF vector, and a cell with an orientation index of 0 would have its long axis aligned perpendicular to the EF vector. The aspect ratio (AR) was determined by the formula: $\text{AR} = \frac{[\text{major axis}]}{[\text{minor axis}]}$ where an increasing aspect ratio indicates a longer and narrower shape.

Live-dead cell counts

Cell culture methods described above were used to seed donor A cells into the ibidi © device cell chambers. After varying EF exposure times and strengths, the media was gently rinsed from chambers with PBS, and cells were stained using a mixture of 1:500 Propidium Iodide stock solution (1mg/ml) (Invitrogen) and 1:500 RNase solution (100mg) (Roche) in PBS for 30 minutes in the dark. The cell chambers were rinsed again gently with PBS, and then 4% glutaraldehyde solution in PBS for 15 minutes to fix the cells, followed by an additional PBS rinsing step. Cells were then

immediately imaged using fluorescence microscopy (Olympus IX51 microscope, equipped with a QImaging micropublisher 3.3 RTV camera and an Olympus U-RFL-T lamp) using a 10x objective, and Qcapture imaging software (Qcapture Pro 6.0).

Immunostaining

Donor A cells were seeded as before then exposed to control conditions (no EF) or a 2V/cm EF for 5 hours within the ibidi© cell chamber. Cells were then washed gently in PBS, fixed in 4% paraformaldehyde at 37°C for 10 minutes and permeabilised using 0.1 wt% Triton X-100 for 5 minutes. A 3% BSA (bovine serum albumin)/PBS blocking solution was added for one hour before incubating the cells with 1:500 anti-vinculin clone hVin1 monoclonal antibody (Sigma Aldrich) in 3% BSA at room temperature for 30 minutes. Cells were then soaked in 3% BSA/PBS solution for 30 minutes, and then washed gently with PBS before incubation with 1:500 anti-mouse IgG-Alexa Fluor 568 secondary antibody (Invitrogen), 1:1000 Alexa Fluor 488 phalloidin (Invitrogen) and 1:1000 Hoechst (Invitrogen) in 3% BSA /PBS for 30 minutes at room temperature. Cells were then again rinsed gently in PBS just prior to high resolution microscopy with an LSR710 confocal microscope (Zeiss) using a 10x objective.

Statistical methods

Averages are presented as mean \pm standard error of the mean. Statistical analysis was performed using GraphPad Prism 6 (La Jolla, CA). The data distribution for donor cells A, B and C for mean values for accumulated distance, euclidean distance, speed of migration, percentage of cells migrating in the direction of the EF and for donor A cells for cell area, cell circularity, AR, and fit ellipse angle were found to be consistent with a Gaussian (normal) distribution when tested with either the D'Agostino & Pearson omnibus or the Shapiro-Wilks normality tests. Only the mean cell viability values for donor A cells at 10 hours of EF stimulation failed both normality tests, however once the mean viability values for 5 V/cm EF stimulation were removed the data was consistent with a Gaussian distribution. Population variances for these mean values were found to be equal using the Brown-Forsythe test for homogeneity. To determine statistical significance a two-way analysis of variance was performed with $P < 0.05$ deemed as significant (**** $P < 0.0001$, *** $P < 0.001$, ** $P < 0.01$). A Bonferroni correction was performed for two-way analysis of variance when comparing MSC donor A data, and a Tukey test was performed for when comparing MSC donor A, B and C data. Similarly, the data distribution for donor D cells for control (static culture) and fluid

flow (6 or 20 $\mu\text{L}/\text{hour}$) conditions at time points of 1, 4 and 8 hours were compared. Mean values were determined for accumulated and euclidean distances, migration speed, percentage of cells migrating in the direction of the fluid flow, cell area, cell circularity, AR, and fit ellipse angle. Measurements of the temperature of the cell migration chamber under control (no EF) or applied EF strengths of 2 or 5 V/cm for up to 18.5 hours were also compared, and statistical significance of these values was determined using a two-way analysis of variance with a Tukey's multiple comparison test with $P < 0.05$ deemed as significant. Additionally, for immunostained cells under either control (no EF) or EF exposed conditions, values were obtained for focal adhesion complexes (FACs) number per cell, FAC area, FAC major and minor axis lengths, and FAC intensity using CellProfiler cell image analysis software version 2.1.1 (www.cellprofiler.org)⁴⁹. These values were found to be consistent

with normal distribution when tested with either the D'Agostino & Pearson omnibus or the Shapiro-Wilks normality tests. Data sets were analysed using a two-tailed paired t test, and statistical significance was set at $P < 0.05$.

Results

Directional migration

In the absence of an EF (control), hBM-MSCs did not show a significant directional migration response (figure 2B, figure 3, figure 4). A highly directional migration response occurred after 0.5 to 3 hours (and persists for up to 15 hours) between 0.5V/cm and 5 V/cm, where cells migrated towards the cathode (figure 2D, E, F, H, J, L, P, figure 3A,B, and figure 4 as labelled). This directional response at field strengths $\geq 0.5\text{V}/\text{cm}$ was found to be significant at

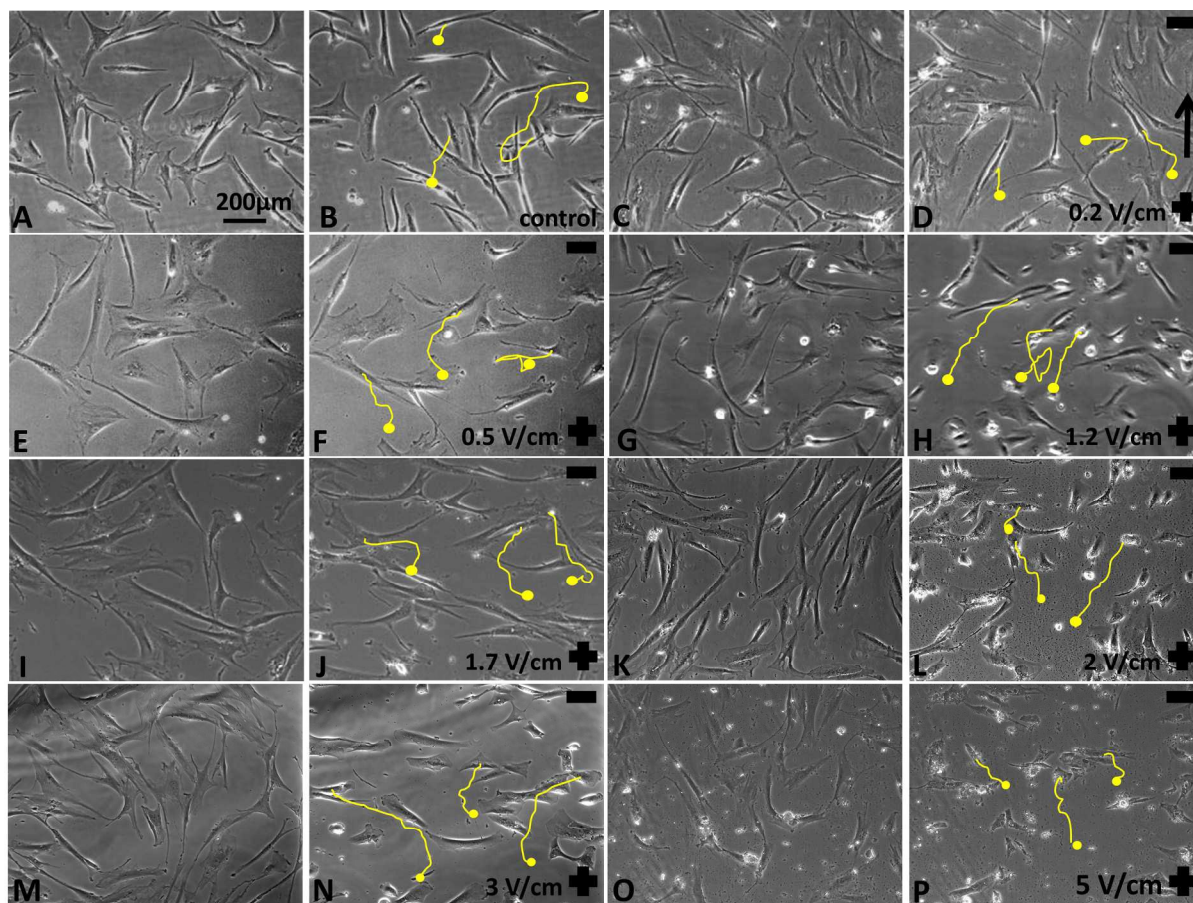


Fig 2. MSCs elongate at ≥ 0.2 V/cm, align perpendicularly to the EF vector at ≥ 0.5 V/cm, and migrate towards the cathode (negative electrode) under EF stimulation. Control (no EF) time 0 (A) and 15 hours (B); 0.2V/cm time 0 (C) and 15 hours (D); 0.5V/cm time 0 (E) and 15 hours (F); 1.2V/cm time 0 (G) and 15 hours (H); 1.7V/cm time 0 (I) and (J) 15 hours; 2V/cm time 0 (K) and (L) 15 hours; 3V/cm time 0 (M) and (N) 15 hours; 5V/cm time 0 (O) and (P) 15 hours. The arrow indicates the direction of cell migration. The migration tracks of a few cells are shown from start (yellow dots) to end of 15 hour study period (yellow lines). Scale bar is shown.

ARTICLE

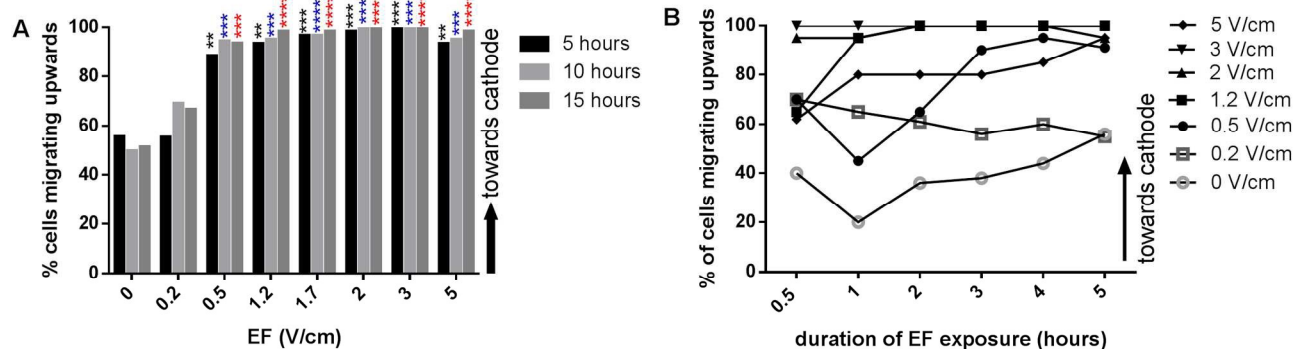


Fig 3. (A) A directional migration response (upwards/ towards the cathode as shown by the arrow) occurs at ≥ 0.5 V/cm for donor A cells. Statistical significance was reached for all time points for EF strengths ≥ 0.5 V/cm when compared to control values. (B) There was a lag-time for donor A cells to show a directional response to EF stimulation, which varied depending on the EF strength; 3 hours for 0.5 V/cm, 1 hour for 1.2 V/cm, within 30 minutes for 2 and 3 V/cm, and 1 hour for 5 V/cm.

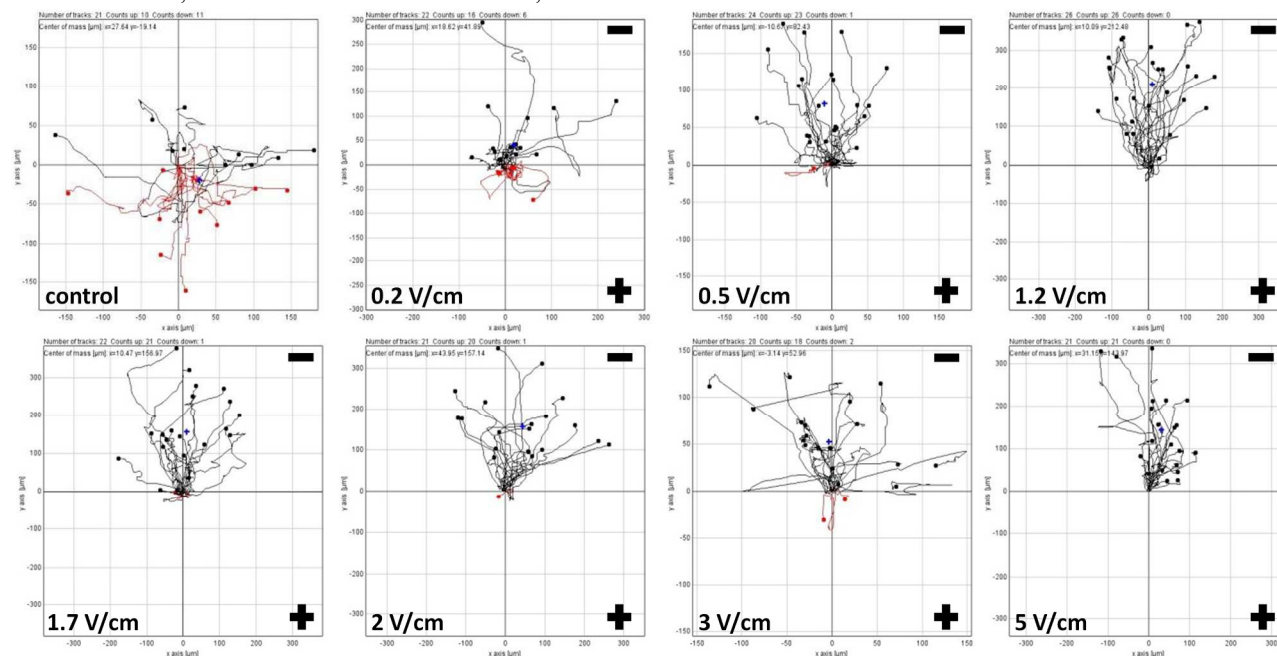


Fig 4. MSCs migrate towards the cathode (negative electrode) under EF stimulation. All plot charts depict migration over a 15 hour period. The blue marker indicates the centre of mass (the average of the x and y coordinates), red colour indicates cell migration over towards the anode, and black colour indicates cell migration towards the cathode.

5, 10 and 15 hours of EF stimulation when compared to the control groups (figure 3A). The directional response of cells to EF stimulation occurred after a lag time, which varied with the strength of EF exposure, and ranged from 3 hours to within 30 minutes from the onset of the EF (figure 3B). At 0.2 V/cm (figure 2D), although there were also not a statistically significant number of cells migrating cathodally, versus anodally (figure 3A), the centre of mass (blue marker (+) figure 4) shows the cells stimulated at 0.2 V/cm

over 15 hours are moving towards the cathode. Passage 7 cells from donor A were stimulated with a 1.2 V/cm EF for 4 hours, and at this time 93% of the cells were migrating towards the cathode. The direction of the EF was then reversed, and cells subsequently began migrating towards the anode. Of sixty cells counted, 15% had changed migration direction in <15 minutes, 30% in <30 minutes, 45% in <45 minutes, 80% in 2 hours, 90% in 2.5 hours, and 100% by 3.5 hours. Donor D cells exposed to continuous fluid flow rates

ARTICLE

of 6 $\mu\text{L}/\text{hour}$ or 20 $\mu\text{L}/\text{hour}$ or static conditions showed no significant differences in migration direction over an 8 hour period (see supplementary figure S1A). There were also no significant differences in the mean values for the various cell morphological parameters under fluid flow conditions (6 $\mu\text{L}/\text{hour}$ at 4 or 8 hours, or 20 $\mu\text{L}/\text{hour}$ at 4 or 8 hours) versus static culture (0 hours of fluid flow stimulation) (see supplementary figure S1B-E). Neither the speeds, euclidean or accumulated distances travelled by cells under 6 or 20 $\mu\text{L}/\text{hour}$ fluid flow or static culture conditions were significantly different at 4 or 8 hours (see supplementary figure S2A-C). The euclidean distance travelled by cells was the only parameter to show any sustained statistical increase over longer time points (similar to those seen in our EF experiments, i.e. 4 or 8 hours) under 20 $\mu\text{L}/\text{hour}$ fluid flow (see supplementary figure S2B). However, the observed delta increases in euclidean distance were significantly smaller than those seen over similar timepoints for an applied EF of 5 V/cm (or lower).

Galvanotropism/ cell morphology

A substantial change in cell morphology in response to EF stimulation was observed (figure 2A-P, figure 5A-D, F-H)). We measured changes in cell alignment to the EF vector (orientation index), cell shape (circularity, aspect ratio) and cell size (attached cell spread area) under EF stimulation (figure 5C, D, F, G).

Cellular alignment, elongation, actin organisation and FACs:

Compared to the control conditions (0 hours) (figure 5A), hBM-MSCs became significantly more elongated with EF exposure (figure 5B,F), and actin stress fibres elongated perpendicularly to the EF vector (figure 5B). Cellular elongation occurred at all time points for 0.2 V/cm, and at 0.5 V/cm, cells were more elongated after 15 hours. At 1.2 V/cm, cells were more elongated at 10 and 15 hours. At 1.7 and 3 V/cm, cells became more elongated at 5 and 10 hours, then at 15 hours, they were less elongated than at earlier time points, but were still more elongated than control conditions (figure 5F). There were significantly more FACs in control cell (no EF) populations versus EF stimulated cells. The FAC area, FAC major and minor axis lengths, and FAC staining

intensity for vinculin in EF-exposed cells was significantly greater than for non EF-exposed cells (see supplementary figure S3A-E). As determined from the orientation index, cells aligned perpendicularly to the applied EF vector at all time points for EF strengths ≥ 0.5 V/cm and ≤ 3 V/cm.

Cell processes: Cells extended lamellopodia towards the cathode whilst undergoing electrotaxis. As the EF strength increased to 2 or 3 V/cm, there was a clear absence of lamellopodia on the anodal side of the cells. After 5 hours of 5 V/cm EF stimulation, no such clear lamellopodia were seen, although cells did migrate small distances towards the cathode (figure 5H).

Control cell populations: In the absence of an EF stimulation (control conditions), cells elongated over time (supplementary figure S4A, although in contrast with cells exposed to EF strengths ≥ 0.5 V/cm and ≤ 3 V/cm, there was no indication of preferential alignment to any axis (supplementary figure S4B). The circularity values of control cells did not change over time (figure S4C). The surface area of the control cells increased with time (supplementary figure S4D), which contrasts to the decrease in attached surface area occurring in cells exposed to EFs ≥ 1.7 V/cm.

Speed and distance of migration

MSCs showed statistically significant increases in migration speed compared to control cells (figure 6A) for 0.2 V/cm at 10 hours, 0.5 V/cm at 15 hours, 1.7 V/cm at 5 and 10 hours, 2 V/cm and 3V/cm at 5, 10 and 15 hours, and 5 V/cm at 10 hours. The fastest migration speeds were noted at 3V/cm EF exposure (for donor A cells). The euclidean metric is the "ordinary" distance between two points that one would measure with a ruler. There was a significant increase in the euclidean distance for EF exposed cells compared to control cells for 0.2 V/cm at 10 and 15 hours, 1.2 V/cm at 10 and 15 hours, and for 1.7 V/cm, 2 V/cm and 3 V/cm at 5, 10 and 15 hours. At 10 hours of 2V/cm EF exposure, cells travelled the furthest euclidean distance for all time points and voltages (figure 6B), and as stated above at this EF strength and duration, cell death was not significant and so

ARTICLE

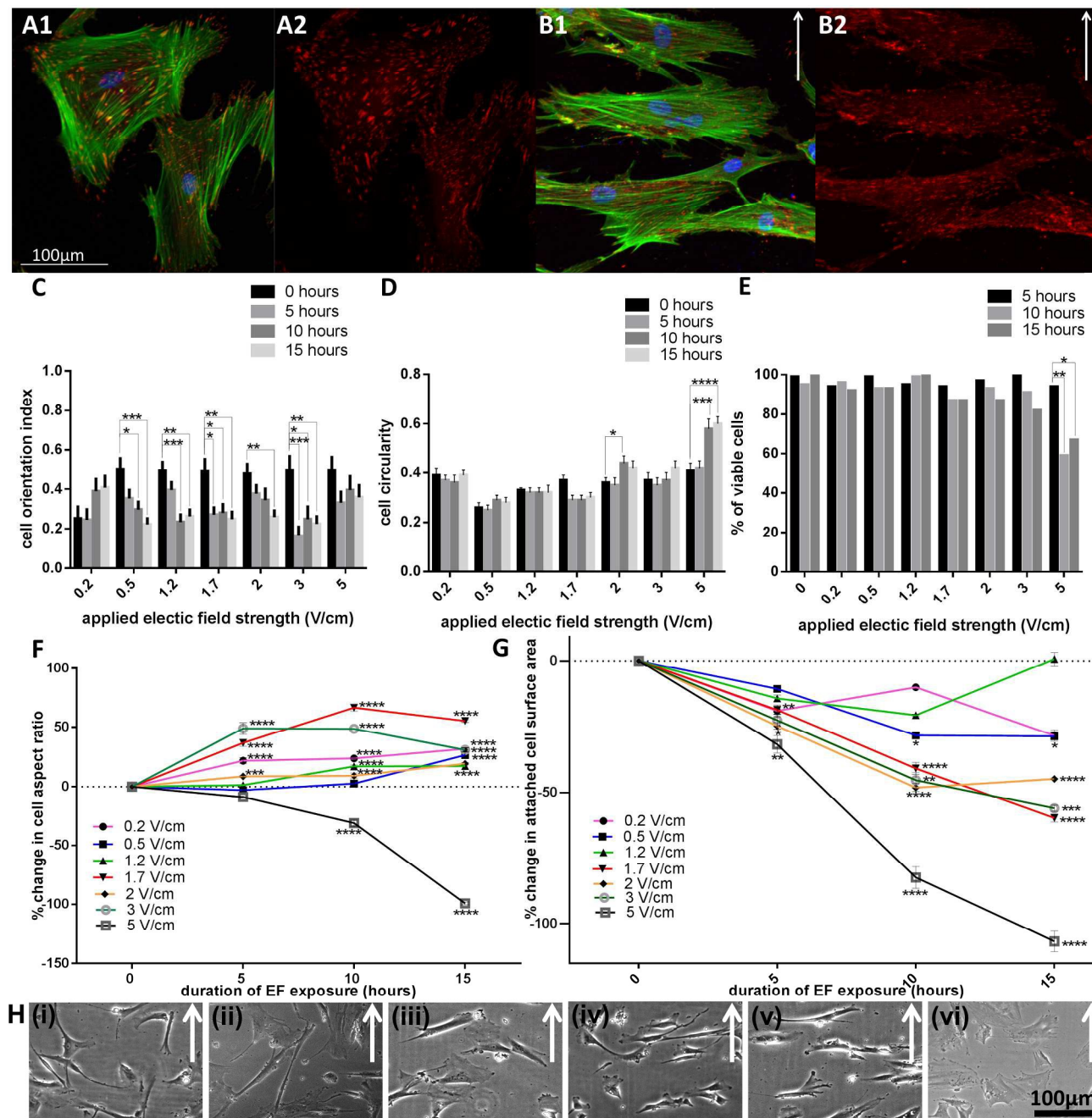


Fig 5. Confocal images indicating focal adhesion complexes (FACs) (A1) and cell morphology (A2) at 15 hours of no EF, and focal adhesion complexes (B1) and cell morphology (B2) with EF exposure. FACs were stained with vinculin (red), actin with phalloidin (green), and DNA with Hoescht (blue). (C) cell orientation with EF exposure. (D) cell circularity with EF exposure (E) cell viability with EF exposure (F) cellular elongation with EF exposure occurred except for at 5 V/cm. (G) The surface area of cell attachment decreased relative to controls (no EF) over time, (H) cell processes were randomly oriented after 5 hours in controls (no EF) (i), and after 5 hours under a 0.5 V/cm EF (ii), there was a clear predilection for cathodally-directed lamellopodia after 5 hours of 1.2 V/cm EF (iii), after 5 hours of 2 V/cm EF (iv) or 3 V/cm EF (v), the extension of cellular processes towards the cathode was marked. Lamellopodia were not seen when cells were exposed to 5 V/cm for 5 hours (vi). The arrows indicate the direction of the cathode. Scale bars are shown.

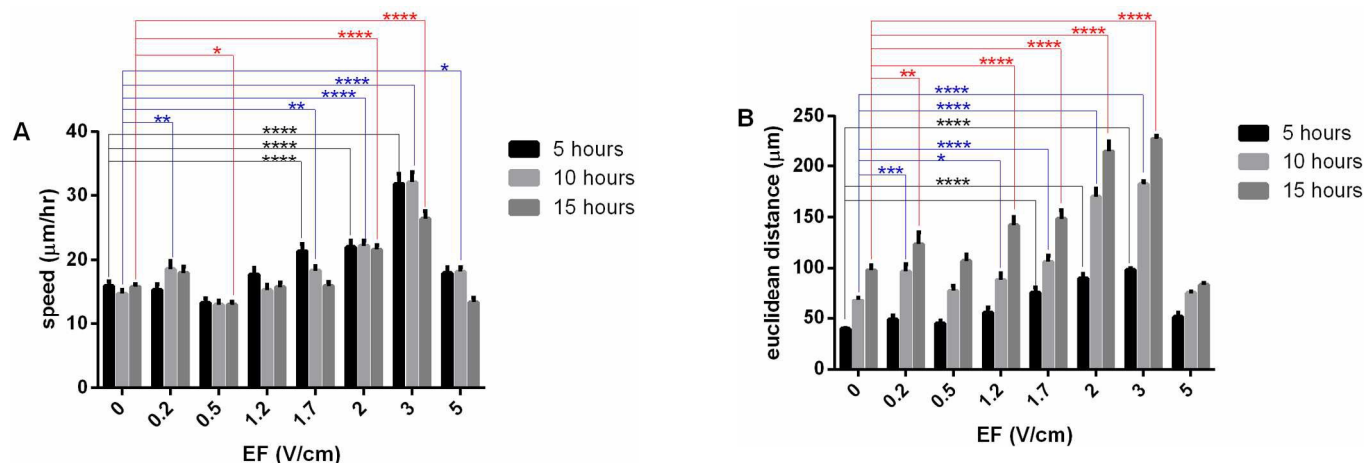


Fig 6. (A) Speed of migration for Donor A cells over the various times shown. There was a significant increase in migration speed for EF exposed cells compared to control cells for 0.2 V/cm at 10 hours, 0.5 V/cm at 15 hours, 1.7 V/cm at 5 and 10 hours, 2 V/cm and 3 V/cm for all time periods shown, and 5 V/cm at 10 hours. (B) euclidean distance travelled for Donor A cells at various times shown. There was a statistically significant increase in euclidean distance for EF exposed cells compared to control cells for 0.2 V/cm at 15 hours, 1.2 V/cm at 10 and 15 hours, and 1.7 V/cm, 2 V/cm and 3 V/cm at all time periods.

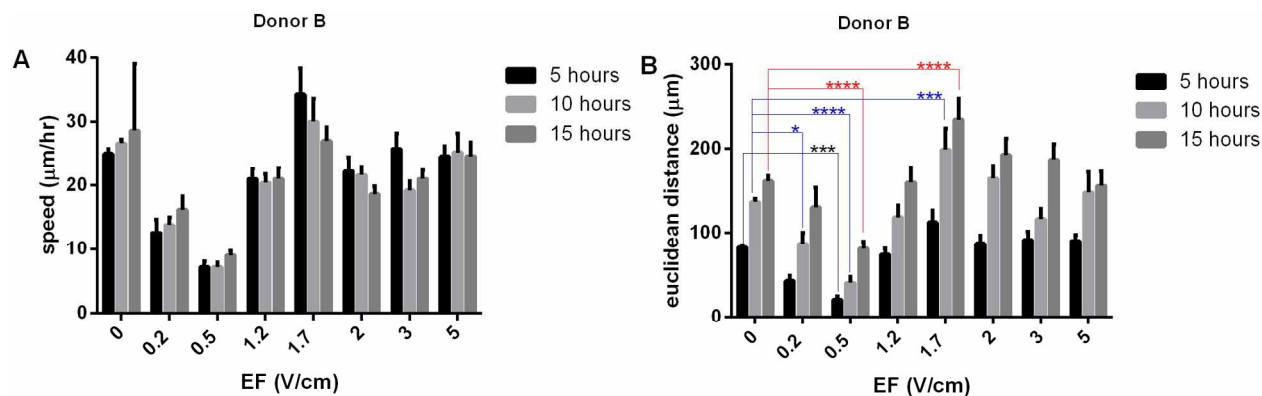


Fig 7. Donor B cells' control and experimental populations did not show significant differences in migration speed (A), but did show differences in (B) euclidean distance (significantly lower at 0.5 V/cm for all time points, and significantly higher for 1.7 V/cm at 10 and 15 hours).

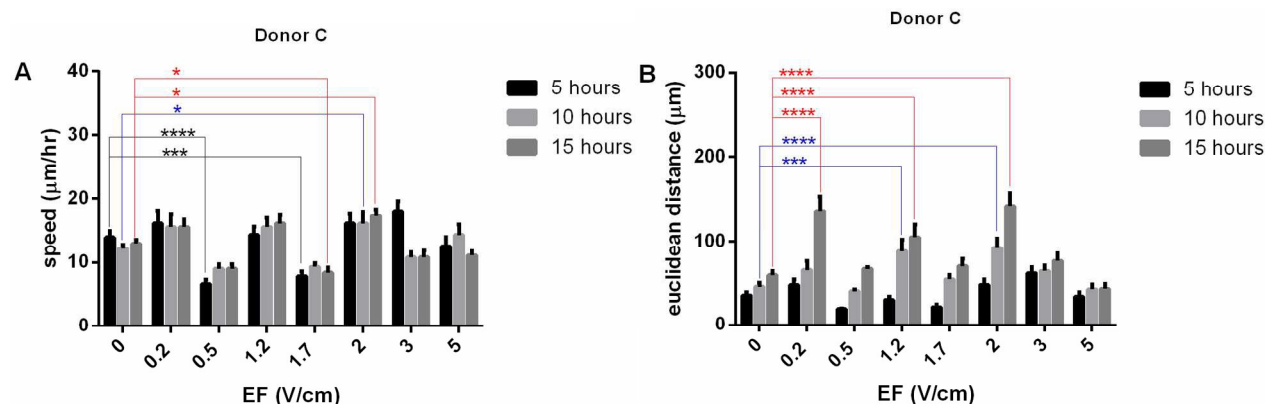


Fig 8. Donor C cells' control and experimental populations showed significant differences in (A) migration speed, and (B) euclidean distance.

the more circular shape seen was not associated with cell viability, and was in fact associated with an increase in the directedness of migration. Accumulated distances travelled (the total cell path travelled in any direction) were significantly increased at 0.5 V/cm (at 15 hours), 2 V/cm (at 10 and 15 hours), 3 V/cm (at 5, 10 and 15 hours), and 5 V/cm (at 15 hours) (supplementary figure S5A).

Donor comparisons

Migration speeds and euclidean distances travelled varied between donors. For donor B cells, migration speeds under EFs were not significantly different to that of controls (figure 7A). However, the rate of migration of the donor B control cells was $\sim 10 \mu\text{m}/\text{hour}$ faster than for control cells from the two other donors. Slower migration speeds relative to controls were found at 0.5 V/cm (5 hours) and 1.7 V/cm (5 hours, 15 hours) for donor C cells (figure 8A), and 0.5 V/cm (15 hours) for donor A cells (figure 6A), although cells maintained highly cathode-directed migration responses. Cells showed fastest migration speeds relative to controls at 3 V/cm for donor A cells (from $\sim 15 \mu\text{m}/\text{hour}$ to $\sim 35 \mu\text{m}/\text{hour}$) (figure 6A), 1.7 V/cm for donor B cells (from $\sim 25 \mu\text{m}/\text{hour}$ to $\sim 35 \mu\text{m}/\text{hour}$) (figure 7A) and 2 V/cm for donor C cells (from $\sim 13 \mu\text{m}/\text{hour}$ to $17 \mu\text{m}/\text{hour}$) (figure 8A). MSCs from different donors showed variable euclidean distances of migration. For donor A cells, the euclidean distances migrated were increased relative to controls for 0.2 V/cm (15 hours),

1.2 V/cm (10, 15 hours), and for all time periods for 1.7 V/cm, 2 V/cm, and 3 V/cm (figure 6B). Euclidean distances travelled for donor C cells were highest at 0.2 V/cm at 15 hours and at 1.2 and 2 V/cm at 10 and 15 hours (figure 8B). Yet for donor B cells, the euclidean distances travelled were decreased relative to controls at 0.2 V/cm (10 hours), 0.5 V/cm (all time periods) and 1.7 V/cm (10, 15 hours) (figure 7B). Under a 5 V/cm EF, donor C cells showed statistical differences to other donor cells, with the directional responses greatly reduced at 5 and 15 hours. Cathodal migration for donor B and C cells after 15 hours of 0.2 V/cm EF was more definitive than for donor A cells. There were no other significant differences in directional response between cell donors, with directionality under EF stimulation being preserved for all donors, as was the lack of directional migration in the absence of an EF (figure 9A-C). There were significant reductions in accumulated distance travelled for donor B cells under EF conditions (0.2, 0.5, 2 and 3 V/cm) compared to controls (supplementary figure S5B). Donor C cells' accumulated distances travelled were highest under 2 V/cm EF stimulation at 10 and 15 hours (supplementary figure S5C). When comparing donors, the accumulated distances were significantly less for donor C compared to donor B cells at 5 and 10 hours (supplementary figure S6A,B), and euclidean distance was also less for donor C compared to donor A cells at 5 hours, and donor C

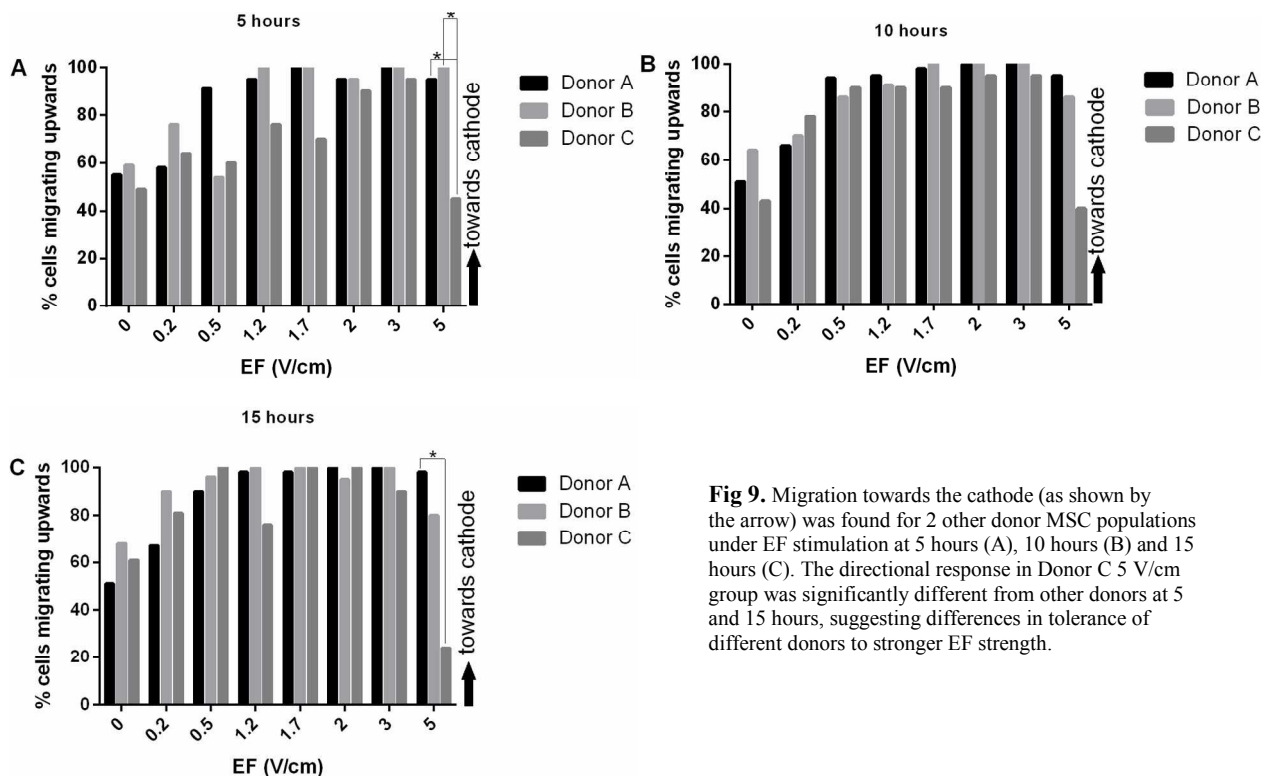


Fig 9. Migration towards the cathode (as shown by the arrow) was found for 2 other donor MSC populations under EF stimulation at 5 hours (A), 10 hours (B) and 15 hours (C). The directional response in Donor C 5 V/cm group was significantly different from other donors at 5 and 15 hours, suggesting differences in tolerance of different donors to stronger EF strength.

versus donor B cells at 10 hours (supplementary figure S7A,B). When comparing the speed, accumulated distance and euclidean distance travelled of the various donor cells, the only statistically significant differences were found at 1.7 V/cm. At this EF strength, consistently lower speed was found for donor C compared to donor B cells at all time periods (supplementary figure S8). One limitation of this study is that there was only one experiment performed for each EF strength for donor B and C cells, and so variations in responses with particular cell culture populations may be somewhat magnified, although as exemplified above, there were significant consistencies in many of the observed behaviours across these donors. The chamber temperatures measured using the infra-red laser gun for control (no EF) and 2 or 5V/cm EFs for up to 18.5 hours did not differ significantly (see supplementary figure S9).

Discussion

We report here a novel adaptation of an ibidi® cell culture device which allowed for multiple simultaneous repeats of control and experimental conditions when determining the effect of EF on cell populations. This medium throughput device increases accuracy by reducing variability in cell populations and experimental conditions by allowing for 6 technical replicates to be performed at once. In addition, we have applied EFs for longer time points and for a larger range of physiological and aphysiological strengths than previously reported with any cell type to form a detailed study of the morphology and kinetics of hBM-MSCs. A wide range of EF strengths is relevant to tissue repair, because *in vivo* EFs of 1-2 V/cm have been measured near the centre of cutaneous wounds, with a lateral declining gradient of EFs strength⁵⁰. Prolonged EF application was also considered important, since colonisation times for cells directed under EF guidance into three-dimensional, highly porous scaffolds with tortuous interconnections could be significant, even for thin scaffolds such as those used for minor defects. By studying a range of EFs, we determined that for hBM-MSCs, there is a 'threshold' EF strength at which directional migration occurred, which varied between donors, as did the effects of EF stimulation on cellular viability, migration rate, migration distance and directionality. Although this static culture model of a 15 hour time period of EF stimulation is close to the maximum time permissible, we were able to highlight differences in donor cell populations.

Table 1. Reported lag times in cellular directional migratory responses to EF stimulation.

Author	Cell type	EF strength (V/cm)	Reported lag time in directional response
^{20b}	CHO cells	3	10-30 minutes
⁵¹	Rabbit corneal endothelial cells	2-10	60 minutes
^{18b}	Fish keratocytes	1	7 minutes
^{18b}	Fish keratocytes	5	4 minutes
^{12d}	Rat osteoblasts	10	5-45 minutes
^{12d}	Rabbit osteoclasts	10	2-10 minutes
^{12d}	Rat osteoblasts	1	>8.6 hours
^{12d}	Rabbit osteoclasts	1	1-2.7 hours
^{26a}	human iP cells	0.3-2	10 minutes
^{17b}	Rat mammary cancer cells	0.5-4	5 minutes
⁵²	Human lung cancer cells	2.25	0 minutes

Directional response

We discovered a consistent definitive cathodal migration response under EFs ≥ 0.5 V/cm and ≤ 3 V/cm for all donors studied, for up to 15 hours. We have shown that the expected electro-osmotic fluid flow rate of 6 μ L/hour does not factor as a stimulation for the directional cell migration, alignment, orientation or other morphological changes seen in hBM-MSCs as a result of EF stimulation. The time for donor A cells to respond with directed migration varied with the EF strength. Other authors have also reported lag times in directional responses, as shown in table 1. It is clear that the lag time for cells to display directional migration varies with the cell type and EF intensity. In the donor A cell population, the directional response occurred more rapidly with increasing EF strengths (at 3 hours for 0.5 V/cm, 1 hour for 1.2 V/cm, and 30 minutes for 2 V/cm and 3 V/cm). However at 5 V/cm, cells showed directed migration after 5 hours. Cells may have been slower to respond to 5 V/cm EF due to deleterious effects of a strong EF, while weaker EFs may take longer to exert their effects on cellular components involved in the directional response. Importantly, we also found that cells took longer or shorter time periods to respond to various EF strengths, depending on the particular donor. The 15 hour study period is important, as it shows that at low EF strengths, directed migration occurs after 10-15 hours, when this was not readily apparent at 5 hours (donor B and C cells). In another study, this long delay in directional migration was also reported; where rat osteoblasts showed no significant directed migration during the first 8.6 hours of stimulation with a

1 V/cm EF, but went on to migrate towards the cathode during the second 8.6 hour study period^{12d}. Our donor A cells displayed directional migration at 0.5 V/cm within 30 minutes of EF exposure, yet donor B and C cells showed a directional response at 0.2 V/cm after 10-15 hours. The threshold EF to induce directional migration of donor A cells was therefore between 0.2 and 0.5 V/cm, and for donor B and C cells was between 0 and 0.2 V/cm. The physiological relevance of these differences is unclear, although the EF threshold at which cells will show a directional response holds some promise in predicting their *in vivo* behaviour. For example, one human lung cancer cell line (proven to be more invasive *in vivo* and *in vitro* than its parent cell line), showed anodal migration at 0.74 V/cm, and even greater directedness at 3.75 V/cm, while its parent cell line did not show a directional response even at 3.75 V/cm⁵². Stronger electrotactic responses have been reported for other highly metastatic cancer cell lines compared to their weakly metastatic counterparts^{17b}, and others have reported immediate directed migration, with no lag period for cancer cells⁵². Whether or not the electrotactic responses of various cells could be used as a way of predicting their *in vivo* behaviour or potentially sorting subpopulations of cells within larger heterogeneous populations remains to be determined. Zhao et al (2011) showed hBM-MSCs migrated directionally between 1 and 0.25 V/cm, and that this directional response was sustained for up to 8 hours, with increased in directedness with increased EF strength²⁷. We found that this directional response could be maintained for nearly double this period of time for 2 of 3 donors, and we also showed an increased directional response with higher EF strength, and for longer duration of EF exposure. It remains to be determined why particular cells migrate towards the cathode (e.g. rat osteoblasts, bovine chondrocytes, bovine vascular endothelial cells, mouse EnSCs, mouse A-MSCs, human ESCs)^{12d, 15, 53} and yet others migrate towards the anode (e.g. rabbit osteoclasts, human osteosarcoma cells, rabbit corneal endothelial cells, rabbit corneal fibroblasts, human vascular endothelial cells)^{12c, d, 44, 51, 53b}. Even more perplexing is why human bone-marrow MSCs would migrate cathodally in the current study and anodally in a previous study²⁷. The literature on human MSC migration direction in response to EFs is sparse. In another report on hA-MSCs²⁸, characteristic elongation was seen at 6V/cm EFs, although migration in either direction was not mentioned. Similar to our findings, cathodal migration of murine adipose-derived stromal

cells²⁹ has been reported, and cathodal migration for other mesenchymal cell types such as chondrocytes¹⁵, ligament fibroblasts⁵⁴, 3T3 fibroblasts⁴³, osteoblasts^{12d, 53b, 53b}, bovine aortic vascular endothelial cells^{53a}, human keratinocytes⁵⁵, and mouse embryonic fibroblasts⁵⁶ has also been reported. In fact, most cell types migrate cathodally, although there are reports of anodal migration for other mesenchymal cell types, including SaOs2 cells^{53b}, human vascular endothelial cells⁴⁴, rabbit corneal endothelial cells⁵¹, and rabbit corneal fibroblasts^{12c}. Although the mechanism of electrotaxis is as yet unclear, these variations in directional response do occur for apparently similar cell types. There is likely to be significant heterogeneity within BM-MSC populations from the same species. This heterogeneity is also apparent from other studies, for example, mouse A-MSCs showed an increase in cathodal directedness, cellular orientation perpendicular to the EF vector, and migration speeds as EF strength increased from 1, 6 and 10 V/cm²⁹. These field strengths have been shown to be deleterious to our hBM-MSCs. In another study, rat epSCs behaved comparably to hBM-MSCs showing cathodal migration from 0.5 to 4 V/cm EFs, which increased with time and EF strength⁵⁷. Human A-MSCs exposed to a 6 V/cm EF showed elongation and alignment within 2 hours, but failed to migrate even after 4 hours²⁸, and human gingival fibroblasts did not migrate under a 10 V/cm EF within 6 hours of exposure, but did align and elongate^{12e}. Similarly, mouse embryonic fibroblasts showed galvanotropism but cathodal migration was only ~ one cell-width in distance after 60 minutes at 10 V/cm. These are strong EFs, however even at progressively lower EFs, responses of these particular cells were even less marked until no significant morphological changes were seen at 1 V/cm for up to 2 hours⁵⁶. From these studies it is clear that even at physiological EF strengths, not all cells will exhibit galvanotropism or galvanotaxis. It is important to note however that an absence of migration confirms an EF influence, as cells migrate randomly in control conditions^{14a, 15, 17b, 18b, 26a, 27, 29, 58}.

Cell viability

Cellular viability under EF stimulation was maintained for at least 5 hours for all EF strengths investigated. Electric field strengths ranging from 0.2 to 3 V/cm did not cause cell death for the 15 hours of the study period. There was a loss of directional response for donor C cells under the strongest EF strength (5 V/cm) within 5 hours of its application. Cell death was thought to be the cause of this, as these cells adopted a circular shape and

lifted from the substrate (data not shown). Both donor A and donor B cells seemed more tolerant of the imposed EFs than donor C cells, as many cells were able to maintain their directional response and attachment to the substrate under a 5 V/cm EF. Live-dead stains confirmed that after 15 hours of 5 V/cm EF exposure approximately 35% of the donor A cell population had died, yet cell tracking data showed that remaining cells were able to maintain directional migration. The extended study period showed that even when cells survive a 5 hour time period at high EF strength, they may go on to die at 10-15 hours (donor C cells, data not shown; and donor A cells between 10-15 hours). In the previously reported study of hBM-MSCs EF stimulation, Zhao et al (2011) showed that cells remained viable after 2 hours exposure to a 6 V/cm EF²⁷, however we can now predict that hBM-MSCs viability would have declined after longer exposure to this EF strength. In other studies, some types of cells are able to elongate, align and migrate under prolonged exposure to EFs as high as 10V/cm. This tolerance to stronger EFs has been demonstrated for rat osteoblast-like cells (4 hours), rabbit osteoclast cells (10 hours)^{12d}, and mouse A-MSCs (6 hours)²⁹, although cell viability studies after EF stimulation were not performed. Poor tolerance to stronger EFs has been shown for mouse embryonic fibroblasts, which suffer significant decreases in cell viability when exposed to 10 V/cm for durations longer than 30 min⁵⁶. We have shown via various experimental measures and theoretical calculations that the heating of cells via the Joule effect does not account for cell death at higher EF strengths, due to the high resistance of the salt bridges and the fact that the channel height in our setup was 400 μ m which allows for rapid heat dissipation. The cell culture chamber was sealed, to protect it from evaporation and contamination. Longer imaging periods have been reported to correlate with a change in pH of the cell migration chamber, and a slight decrease in EF strength⁵⁹, and Allen et al. (2013) showed that while fish keratocytes' electrotactic response was present at a pH of 6.2, it was lost at a pH of 5.8^{18b}. Given that the electrotactic response was preserved for the 15 hour period, and that cells maintained their speed of migration throughout the experiment, pH is unlikely to be a factor in the cell death. Additionally, the pH was measured at the beginning and completion of EF exposure and even after 15 hours of 5 V/cm EF exposure, and it was found to be consistent. The cause of cell death was thought to be due to

lack of media exchange resulting in nutrient depletion and loss of ions from the culture media.

Morphological change

For all cells exposed to an EF, morphological differences were found between control and experimental populations, which were most obvious at EF strengths ≥ 0.5 V/cm and ≤ 3 V/cm EF; where cells elongated and showed perpendicular alignment to the applied EF vector (or alignment parallel to the x-axis). It is important to highlight that under an applied EF, cells elongated in the direction of the x-axis, and yet migrate parallel to the y-axis. We also found a trend for cells to become progressively more aligned with the x-axis over a longer time period and with stronger EF strengths (between ≥ 0.5 V/cm and ≤ 3 V/cm). While Zhao et al (2011) did not discuss changes in hBM-MSCs morphology under EF stimulation, many other cell types have been shown to respond to direct current EFs by not only increasing motility and displaying directed migration, but also exhibiting galvanotropism^{15, 17d, 20b, 28-29, 43, 51, 60}. After 5 hours exposure to a 2V/cm EF, we found most actin filaments were oriented perpendicular to the EF vector, and parallel to the long axis of the cell. In other studies, EF exposure consistently produces changes to the actin cytoskeleton similar to those we have reported, for example human umbilical vein endothelial cells⁴⁴, rat neonatal cardiomyocytes⁶¹, mouse A-MSCs²⁹, hA-MSCs²⁸, and CHO cells⁶². Interestingly, unlike other cell types mentioned, CHO cells elongated and aligned their long axis parallel rather than perpendicular to the EF vector^{20b}. Human trophoblastic cells showed similar actin elongation as well as increased focal adhesion kinase (FAK) phosphorylation⁶³. In cathodally migrating cells, cathodal polarisation of F-actin has also been reported (human lung adenocarcinoma cells⁶⁴, CHO cells^{20b}, bovine corneal epithelial cells⁶⁵, rat embryonic NSCs^{20c}, human retinal pigment epithelial cells^{18g}, and rat epidermal stem cells⁵⁷). While clear and characteristic changes to the actin cytoskeleton occurred in hBM-MSCs, we did not see polarisation of actin towards the cathode. The leading edge of the cell is known to involve PI3 kinase dependent pathways signalling to the protruding actin network, which may predominate in orienting the cell and directing it towards the cathode¹⁶. Inhibition of MAP kinase signaling inhibited leading edge (cathodal) F-actin polarisation and directional migration in bovine corneal epithelial cells⁶⁵. Inhibition of the Arp2/3

complex (a major component of the actin cyto-skeleton) slowed galvanotaxis of fish keratocytes and their fragments, although migration remained highly directional¹⁶. Amoebal cells (undergoing cathodal migration) showed cathodal localisation of proteins of the PI3K and GCase-mediated signaling pathways, which was inhibited with an F-actin polymerization inhibitor⁶⁶. Rat epidermal stem cells also showed reduced cathodal migration when treated with the same F-actin polymerization inhibitor⁵⁷. In conjunction with actin filament alignment and elongation, we found distinct focal adhesions at the ends of actin filaments. Others have reported actin alignment with foci of vinculin near the cell edges or in the direction of cell migration (in human SaOS-2 cells and rat calvarial osteoblasts^{53b}, rabbit corneal fibroblasts^{12c}, and rabbit corneal endothelial cells⁵¹). There was no clear polarisation of FACs in our cells after 5 hours of 2 V/cm EF, and fewer FACs per cell were found in compared to control cells (no EF), correlating with the reduction in attached cell area in EF stimulated cells. Importantly, we found significant enlargement, elongation and increased staining intensity of focal adhesion complexes with EF stimulation. Our study demonstrates that for hBM-MSCs, morphological changes change in accordance with the strength and duration of the applied EF. Cells tended to become more elongated and more aligned with the x-axis at increasing EF strength until they were subjected to longer durations of 5 V/cm stimulation, which resulted in a dramatic increase in circularity and concurrent decrease in attached surface area as they died and lifted away from the substrate. Similar to our findings, other authors have reported increased cell length with EF stimulation; an increase of 45% after 4 hours was reported for human A-MSCs using a 6 V/cm EF²⁸, and an increase in 11% after 1 hour at 4 V/cm for quail embryonic fibroblasts^{60a}, and distinct elongated morphology after 3 hours of exposure to a 3 V/cm EF in 76% of CHO cell^{20b}. Zhao et al. (2012) reported that one particular cell line of mouse EnSC elongated significantly with EF exposure, while another 2 cell lines did not change shape^{53c}. The reasons why cells elongate and align perpendicularly under EF stimulation is hypothesised to be to minimize the voltage drop across themselves^{60b, 67}, although the changes in membrane potential occurring with EF stimulation are as yet unclear. Our study shows conclusively that this perpendicular orientation becomes increasingly more prevalent as the EF strength increases, correlating with a reduction in the voltage drop across the cell with the increase in

cell length parallel to the EF. In terms of mechanism, it has been suggested that an EF parallel to the surface of a cell should redistribute charged macromolecules that are free to move in the cell membrane^{18h}. A uniform EF will be distorted by the highly resistant cell membrane, and the anode-facing cell membrane will hyperpolarize (become more negative) and the cathode-facing side will depolarise (become less negative)^{12a}. A negatively charged mobile macromolecule will move to the cathodal side of the cell if its zeta potential is less negative than that of the cell surface, and if not, it will move to the anodal side^{18f}. Indeed, charged membrane proteins such as Concanavalin A receptors^{18i, 68}, acetylcholine receptors^{18j, 68}, and Fc-epsilon receptors^{18k} will migrate around the cell membrane in response to EF application. The lag time for cells to respond to EFs supports the electrophoresis or electro-osmosis of membrane proteins as part of the mechanistic response, particularly as switching the direction of the EF is also followed by a lag time of 5-10 minutes for fish keratocytes^{18b}, 0.5 to 2 hours for rat osteoblasts, or 3-10 minutes for rabbit osteoclasts^{12d}, and 15 minutes for mouse endothelial progenitor cells^{53c}, an immediate response for rat NSCs^{20c}, 10 minutes for human NSCs^{26b}, and 15 minutes for mouse EnSCs^{53c}, after which cells begin migrating in the opposite direction. Zhao et al (2011) reported hBM-MSCs reversed their direction of migration when the EF direction was also reversed, however the lag time for cells to respond to this change in EF direction was not quantified²⁷. We found for a 1.2V/cm EF, once the direction of the EF was changed, there was a time-dependent reversal of the donor A cell population migrating towards the new cathode. A subpopulation of cells reversed direction within 15 minutes, and many cells took longer, although 100% of counted cells were migrating towards the new cathode by 3.5 hours after EF direction reversal. This heterogeneous response in the time for cells to respond to EF directional change may reflect individual variations in cells such as the number, size and maturity of focal adhesion complexes, the cell's size and attached surface area, the distribution, and size and charge of membrane proteins, and the time to retract and reorient lamellopodia. Indeed, Arocena et al. (2010) showed that rat NSCs migrated towards the cathode, with most cellular protrusions oriented towards the cathode, and when the EF was reversed, most cells retracted protrusions towards the former cathode and formed new protrusions towards the new cathode⁶⁹. Increasing the strength of the EF would likely decrease the time

with which the cell population would respond to a reversal in EF direction, due at least in part to more rapid initial electrophoresis or electroosmosis of membrane proteins. Exactly how the movement of membrane proteins leads to changes in the cytoskeleton and an electrotactic response is unclear. Many authors have described in conjunction with elongation and alignment to the EF vector, cells undergoing electrotaxis have distinct, active membrane protrusions. Chang et al. (1996) reported rabbit corneal endothelial cells showed anodal migration, with active extensions of ruffled membranes and lamellopodia on their anode-facing sides, and retraction of ruffled membranes and lamellopodia along the cathode-facing sides of the same cells⁵¹. Similarly, embryonic quail fibroblasts exhibiting cathodal electrotaxis extended lamellopodia toward the negative pole, and all anode-facing processes eventually retracted^{60a}. Human keratinocytes became fan-shaped cells and had active membrane protrusions on the leading edge of cells undergoing cathodal electrotaxis⁷⁰. Prominent lamellopodia were also present on the cathodal sides of rat osteoblasts^{12d}, bovine chondrocytes¹⁵, and mouse EnSCs^{53c} undergoing cathodal migration. Anodally-directed lamellopodia (from leading edge or from both ends of long axis) and anodal migration was seen in rat mammary cancer cells^{17b}, with similar findings reported for rabbit osteoclasts^{12d}, human SaOS-2 cells^{53b}, and human retinal pigment epithelial cells⁷¹ undergoing anodal migration. We also found that hBM-MSCs extended lamellopodia towards the cathode as they migrated. Most cellular processes were directed towards the cathode after 5 hours of 1.2 V/cm EF stimulation, and there were very few (if any) anodally-directed lamellopodia after 5 hours of 2 V/cm EF stimulation. The lack of anodal processes, cellular elongation and cathodally-directed lamellopodia created a tendency for the cells to become fan-shaped, as reported by others, and the fan-shapes became more elongated as the EF intensity increased up to 3V/cm. At 5 V/cm after 5 hours, cells were not significantly more elongated or more circular compared to themselves at time 0, and although cells migrated directionally towards the cathode, euclidean distances travelled were very small, and there were no obvious cellular processes involved in this directional response.

Migration speeds and distances

When the migration speeds attained at the 5, 10 and 15 hour time points were averaged, we found that donor A cells' migration speeds were $15.5 \pm 0.6 \mu\text{m/hr}$ in the absence of an EF, increasing

relative to control speeds by 1.2 fold at 1.7 V/cm, 1.4 fold at 2 V/cm and 1.9 fold at 3 V/cm EF. Migration speeds were fastest for donor A cells at 3 V/cm, 1.7 V/cm for donor B cells and 2 V/cm for donor C cells. The furthest euclidean distances travelled (indicating highly directed migration) was 2 V/cm for donor A cells, 1.7 V/cm for donor B cells and 2 V/cm for donor C cells. Although there was variability in responses with regard to the speeds and migration distances travelled for the different donors under the same EF strengths, the directional response was highly preserved under EF strengths that did not lead to cell death. In a study by Zhao et al. (2011), passage 3 hBM-MSCs migrated at $32 \pm 1 \mu\text{m/hr}$ in the absence of an EF, increasing relative to control speeds by 1.3 fold under a 2 V/cm EF, correlating well with our findings. In this same study, migration speeds were found to decrease as passage number increased for control and EF-exposed cells²⁷. All cells in our current study were consistently either passage 6 or 7, an important factor in minimising variability in migration speeds²⁷. Hammerick et al. showed that mouse A-MSCs migration speeds were increased relative to controls (no EF) by 1.9 fold, 5 fold, and 10 fold for EF strengths of 1, 6 and 10 V/cm respectively. Mouse osteoblasts were also found to migrate even faster than mouse A-MSCs under the same EF stimulation²⁹. We have also shown variability in cell viability to strong EFs in different donors, and variability in the migration speeds of different donors to the same EF strengths, highlighting the need to tailor electrical stimulation to the individual. Other studies continue to highlight the disparate results seen with different cell types with respect to migration speeds, but the majority of reports show that speeds increase with EF stimulation, in a dose-dependent manner (see supplementary materials- table S4).

Conclusions

In this study we have shown that for highly selected (STRO-1^{high}/VCAM-1⁺) hBM-MSC populations there were some important broad consistent responses to EF stimulation, including sustained cathodally-directioned migration for all hBM-MSCs at $\geq 0.5 \text{ V/cm}$, and dose and time-dependent directional and morphological responses. Depending upon the strength and duration of the applied EF, hBM-MSCs showed repeatable and hence predictable changes in speed, morphology, alignment and directedness of migration. This suggests that cellular behaviours may be manipulated with respect to the direction, number, rate

and type of cells under investigation. Yet even for hMSCs from different donors of the same species there is variability in the response, highlighting the need to optimise conditions for the particular species and cell type. The outcomes of this study suggests that the optimisation of applied electrical stimulation parameters including frequency, intensity, polarity and duration may all be important factors to consider when influencing cells with EFs. Given its clear impact on cellular behaviours important to tissue engineering applications, imposing EFs in a controlled manner may prove to be a useful tool, particularly in the colonisation of scaffolds with potentially therapeutic MSCs in a directed and controlled manner, whilst ensuring cellular viability is maintained. The use of weak EFs over extended periods for in vivo and in vitro therapeutic applications warrants further investigation.

Acknowledgements

The authors would like to thank Miss Li-Yen Wong and Dr Nick Glass from the Tissue Engineering and Microfluidics Laboratory at Australian Institute for Bioengineering & Nanotechnology, The University of Queensland, for her assistance with confocal imaging, and Professor Michael Holland, Director of Research at the University of Queensland, School of Veterinary Science, for discussions regarding this project. This work was performed in part at the University of Queensland node of the Australian National Fabrication Facility, a company established under the National Collaborative Research Infrastructure Strategy to provide nano and micro-fabrication facilities for Australia's researchers. This study was financially supported by the School Of Veterinary Science at the University of Queensland, by The John and Mary Kibble Trust, and by the Australian Institute of Bioengineering and Nanotechnology. J.E.F. is supported by an ARC DECRA Fellowship (DE13010098). The authors have no financial or personal relationship with other people or organisations that could inappropriately influence this work.

Notes and references

Author affiliations:

¹ Tissue Engineering and Microfluidics Laboratory, Australian Institute for Bioengineering & Nanotechnology, The University of Queensland, St. Lucia, Qld 4072, Australia.

²The School of Veterinary Science, The University of Queensland, Gatton Campus, Qld 4343, Australia

³ Centre for High Performance Polymers, Australian Institute for Bioengineering & Nanotechnology, The University of Queensland, St. Lucia, Qld 4072, Australia

⁴ The School of Chemical Engineering, The University of Queensland, Brisbane, Queensland, Australia.

⁵Manufacturing Flagship, CSIRO, Clayton, Victoria, Australia.

* Corresponding Author: Professor Justin J. Cooper-White, email: j.cooperwhite@uq.edu.au

† Electronic Supplementary Information (ESI) available: [details of any supplementary information available should be included here]. See DOI: 10.1039/b000000x/

Literature Cited

- (a) C. Bassett, R. Pawluk, R. Becker, Effects of electric currents on bone *in vivo*. *Nature* 1964, 204. 652-654; (b) M. Kryszewski, Fifty years of study of the piezoelectric properties of macromolecular structural biologic materials. *Acta Phys. Pol.* 2004, A 105. 389-408; (c) R. B. Borgens, L. F. Jaffe, M. J. Cohen, Large and persistent electrical currents enter the transected lamprey spinal cord. *Proceedings of the National Academy of Sciences of the United States of America* 1980, 77. 1209-13; (d) M. Zuberi, P. Liu-Snyder, A. Ul Haque, D. M. Porterfield, R. B. Borgens, Large naturally-produced electric currents and voltage traverse damaged mammalian spinal cord. *Journal of biological engineering* 2008, 2. 17, DOI: 10.1186/1754-1611-2-17; (e) K. B. Hotary, K. R. Robinson, Endogenous electrical currents and voltage gradients in *Xenopus* embryos and the consequences of their disruption. *Dev Biol* 1994, 166. 789-800, DOI: 10.1006/dbio.1994.1357; (f) R. Shi, and Borgens, R.B., Three-dimensional gradients of voltage during development of the nervous system as invisible coordinates for the establishment of embryonic pattern. *Dev. Dyn* 1995, 202. 101-114; (g) B. Song, M. Zhao, J. V. Forrester, C. D. McCaig, Electrical cues regulate the orientation and frequency of cell division and the rate of wound healing in vivo. *Proceedings of the National Academy of Sciences of the United States of America* 2002, 99. 13577-82, DOI: 10.1073/pnas.202235299; (h) L. F. Jaffe, J. W. Vanable, Jr., Electric fields and wound healing. *Clin Dermatol* 1984, 2. 34-44; (i) M. Chiang, K. R. Robinson, J. W. Vanable, Jr., Electrical fields in the vicinity of epithelial wounds in the isolated bovine eye. *Experimental eye research* 1992, 54. 999-1003; (j) K. B. Hotary, Robinson, K.R., Evidence of a role for endogenous electrical fields in chick

- embryo development. *Development* 1992, 114. 985-996; (k) B. Reid, B. Song, C. D. McCaig, M. Zhao, Wound healing in rat cornea: the role of electric currents. *Faseb J* 2005, 19. 379-86, DOI: 10.1096/fj.04-2325com; (l) R. B. Borgens, J. W. Vanable, Jr., L. F. Jaffe, Bioelectricity and regeneration: large currents leave the stumps of regenerating newt limbs. *Proc Natl Acad Sci U S A* 1977, 74. 4528-32; (m) R. O. Becker, The bioelectric factors in amphibian-limb regeneration. *J Bone Joint Surg Am* 1961, 43-A. 643-56; (n) C. D. McCaig, A. M. Rajniecek, B. Song, M. Zhao, Controlling cell behavior electrically: current views and future potential. *Physiol Rev* 2005, 85. 943-78, DOI: 10.1152/physrev.00020.2004; (o) C. D. McCaig, B. Song, A. M. Rajniecek, Electrical dimensions in cell science. *Journal of cell science* 2009, 122. 4267-76, DOI: 10.1242/jcs.023564; (p) M. H. Shamos, L. S. Lavine, M. I. Shamos, Piezoelectric effect in bone. *Nature* 1963, 197. 81; (q) S. Kanno, Oda, N., Abe, M., Saito, S., Hori, K., Handa, Y., Tabayashi, K., Sato, Y., Establishment of a simple and practical procedure applicable to therapeutic angiogenesis. *Circulation* 1999, 99. 2682-2687.
2. (a) A. J. Grodzinsky, H. Lipshitz, M. J. Glimcher, Electromechanical properties of articular cartilage during compression and stress relaxation. *Nature* 1978, 275. 448-50; (b) B. Schmidt-Rohlfing, U. Schneider, H. Goost, J. Silny, Mechanically induced electrical potentials of articular cartilage. *Journal of biomechanics* 2002, 35. 475-82.
3. E. Fukada, I. Yasuda, ON THE PIEZOELECTRIC EFFECT OF BONE. *Journal of the Physical Society of Japan* 1957, 12. 1158-1162, DOI: 10.1143/jpsj.12.1158.
4. D. Pienkowski, S. R. Pollack, The origin of stress-generated potentials in fluid-saturated bone. *Journal of orthopaedic research : official publication of the Orthopaedic Research Society* 1983, 1. 30-41, DOI: 10.1002/jor.1100010105.
5. (a) C. Goldstein, S. Sprague, B. A. Petrisor, Electrical stimulation for fracture healing: current evidence. *Journal of orthopaedic trauma* 2010, 24 Suppl 1. S62-5, DOI: 10.1097/BOT.0b013e3181cdde1b; (b) M. Griffin, A. Bayat, Electrical stimulation in bone healing: critical analysis by evaluating levels of evidence. *Eplasty* 2011, 11. e34; (c) K. Kohata, S. Itoh, S. Takeda, M. Kanai, T. Yoshioka, H. Suzuki, K. Yamashita, Enhancement of fracture healing by electrical stimulation in the comminuted intraarticular fracture of distal radius. *Bio-medical materials and engineering* 2013, 23. 485-93, DOI: 10.3233/bme-130774; (d) A. Saxena, L. A. DiDomenico, A. Widtfeldt, T. Adams, W. Kim, Implantable electrical bone stimulation for arthrodeses of the foot and ankle in high-risk patients: a multicenter study. *The Journal of foot and ankle surgery : official publication of the American College of Foot and Ankle Surgeons* 2005, 44. 450-4, DOI: 10.1053/j.jfas.2005.07.018; (e) R. K. Aaron, D. M. Ciombor, B. J. Simon, Treatment of nonunions with electric and electromagnetic fields. *Clinical orthopaedics and related research* 2004. 21-9.
6. (a) M. Akai, H. Oda, Y. Shirasaki, T. Tateishi, Electrical stimulation of ligament healing. An experimental study of the patellar ligament of rabbits. *Clinical orthopaedics and related research* 1988. 296-301; (b) Y. Lin, R. Nishimura, K. Nozaki, N. Sasaki, T. Kadosawa, N. Goto, M. Date, A. Takeuchi, Effects of pulsing electromagnetic fields on the ligament healing in rabbits. *The Journal of veterinary medical science / the Japanese Society of Veterinary Science* 1992, 54. 1017-22.
7. L. Lippiello, D. Chakkalakal, J. F. Connolly, Pulsing direct current-induced repair of articular cartilage in rabbit osteochondral defects. *Journal of orthopaedic research : official publication of the Orthopaedic Research Society* 1990, 8. 266-75, DOI: 10.1002/jor.1100080216.
8. D. M. Ciombor, R. K. Aaron, S. Wang, B. Simon, Modification of osteoarthritis by pulsed electromagnetic field--a morphological study. *Osteoarthritis and cartilage / OARS, Osteoarthritis Research Society* 2003, 11. 455-62.
9. S. T. Sutbeyaz, N. Sezer, B. F. Koseoglu, The effect of pulsed electromagnetic fields in the treatment of cervical osteoarthritis: a randomized, double-blind, sham-controlled trial. *Rheumatology international* 2006, 26. 320-4, DOI: 10.1007/s00296-005-0600-3.
10. A. Negm, A. Lorbergs, N. J. Macintyre, Efficacy of low frequency pulsed subsensory threshold electrical stimulation vs placebo on pain and physical function in people with knee osteoarthritis: systematic review with meta-analysis. *Osteoarthritis and cartilage / OARS, Osteoarthritis Research Society* 2013, 21. 1281-9, DOI: 10.1016/j.joca.2013.06.015.

11. X. Yuan, D. E. Arkonac, P. H. Chao, G. Vunjak-Novakovic, Electrical stimulation enhances cell migration and integrative repair in the meniscus. *Scientific reports* 2014, *4*. 3674, DOI: 10.1038/srep03674.
12. (a) K. R. Robinson, The responses of cells to electrical fields: a review. *J Cell Biol* 1985, *101*. 2023-7; (b) H. K. Soong, W. C. Parkinson, S. Bafna, G. L. Sulik, S. C. Huang, Movements of cultured corneal epithelial cells and stromal fibroblasts in electric fields. *Invest Ophthalmol Vis Sci* 1990, *31*. 2278-82; (c) H. K. Soong, W. C. Parkinson, G. L. Sulik, S. Bafna, Effects of electric fields on cytoskeleton of corneal stromal fibroblasts. *Curr Eye Res* 1990, *9*. 893-901; (d) J. Ferrier, S. M. Ross, J. Kanehisa, J. E. Aubin, Osteoclasts and osteoblasts migrate in opposite directions in response to a constant electrical field. *J Cell Physiol* 1986, *129*. 283-8, DOI: 10.1002/jcp.1041290303; (e) S. Ross, Morphological responses of cells to exogenous ionic currents. *Annu Int Conf IEEE Eng Med Biol* 1990, *12*. 1570-1571; (f) R. Nuccitelli, in *Advances in Molecular and Cell Biology*, ed. R. M. Kenneth. Elsevier, 1988, vol. Volume 2, pp 213-233; (g) C. D. McCaig, A. M. Rajnicek, B. Song, M. Zhao, *Controlling Cell Behavior Electrically: Current Views and Future Potential*. 2005; Vol. 85, p 943-978.
13. M. Zhao, J. Penninger, R. R. Isseroff, Electrical Activation of Wound-Healing Pathways. *Advances in skin & wound care* 2010, *1*. 567-573, DOI: 10.1089/9781934854013.567.
14. (a) F. Lin, F. Baldessari, C. C. Gyenge, T. Sato, R. D. Chambers, J. G. Santiago, E. C. Butcher, Lymphocyte electrotaxis in vitro and in vivo. *J Immunol* 2008, *181*. 2465-71; (b) M. E. Mycielska, M. B. Djamgoz, Cellular mechanisms of direct-current electric field effects: galvanotaxis and metastatic disease. *Journal of cell science* 2004, *117*. 1631-9, DOI: 10.1242/jcs.01125.
15. P. H. Chao, R. Roy, R. L. Mauck, W. Liu, W. B. Valhmu, C. T. Hung, Chondrocyte translocation response to direct current electric fields. *Journal of biomechanical engineering* 2000, *122*. 261-7.
16. Y. Sun, D. Hao, J. Gao, R. Zhao, M. Zhao, A. Mogilner, Keratocyte fragments and cells utilise competing pathways to move in opposite directions in an electric field. *Current Biology* 2013, *23*. 569-574.
17. (a) H. Bai, J. V. Forrester, M. Zhao, DC electric stimulation upregulates angiogenic factors in endothelial cells through activation of VEGF receptors. *Cytokine* 2011, *55*. 110-5, DOI: 10.1016/j.cyto.2011.03.003; (b) J. Pu, C. D. McCaig, L. Cao, Z. Zhao, J. E. Segall, M. Zhao, EGF receptor signalling is essential for electric-field-directed migration of breast cancer cells. *Journal of cell science* 2007, *120*. 3395-403, DOI: 10.1242/jcs.002774; (c) Y. S. Sun, S. W. Peng, K. H. Lin, J. Y. Cheng, Electrotaxis of lung cancer cells in ordered three-dimensional scaffolds. *Biomicrofluidics* 2012, *6*. 14102-1410214, DOI: 10.1063/1.3671399; (d) M. B. A. Djamgoz, M. Mycielska, Z. Madeja, S. P. Fraser, W. Korohoda, Directional movement of rat prostate cancer cells in direct-current electric field: involvement of voltagegated Na⁺ channel activity. *J Cell Sci* 2001, *114*. 2697-705; (e) Z. Siwy, M. E. Mycielska, M. B. Djamgoz, Statistical and fractal analyses of rat prostate cancer cell motility in a direct current electric field: comparison of strongly and weakly metastatic cells. *Eur Biophys J* 2003, *32*. 12-21, DOI: 10.1007/s00249-002-0267-6; (f) C. D. McCaig, M. Zhao, Physiological electrical fields modify cell behaviour. *Bioessays* 1997, *19*. 819-26, DOI: 10.1002/bies.950190912; (g) E. Wang, Y. Yin, M. Zhao, J. V. Forrester, C. D. McCaig, Physiological electric fields control the G1/S phase cell cycle checkpoint to inhibit endothelial cell proliferation. *Faseb J* 2003, *17*. 458-60, DOI: 10.1096/fj.02-0510fje; (h) J. Hang, Kong, L., Gu, J.W., Adair, T.H., VEGF gene expression is upregulated in electrically stimulated rat skeletal muscle. *Am. J. Physiol* 1995, *269*. H1827-H1831; (i) B. Song, Y. Gu, J. Pu, B. Reid, Z. Zhao, M. Zhao, Application of direct current electric fields to cells and tissues in vitro and modulation of wound electric field in vivo. *Nature protocols* 2007, *2*. 1479-89, DOI: 10.1038/nprot.2007.205.
18. (a) K. S. Fang, Ionides, E., Oster, G., Nuccitelli, R. and Isseroff, R. R. , Epidermal growth factor receptor relocalization and kinase activity are necessary for directional migration of keratinocytes in DC electric fields. *J. Cell Sci* 1999, *112*; (b) G. M. Allen, A. Mogilner, J. A. Theriot, Electrophoresis of cellular membrane components creates the directional cue guiding keraotocyte galvanotaxis. *Current Biology* 2013, *23*. 560-558; (c) M. Zhao, A. Dick, J. V. Forrester, C. D. McCaig, Electric field-directed cell motility involves up-regulated

- expression and asymmetric redistribution of the epidermal growth factor receptors and is enhanced by fibronectin and laminin. *Mol Biol Cell* 1999, 10. 1259-76; (d) D. W. Tank, W. J. Fredericks, L. S. Barak, W. W. Webb, Electric-field redistribution and post-field relaxation of low density lipoprotein receptors on cultured human fibroblasts. *The Journal of cell biology* 1985, 101. 148-157; (e) M. J. Brown, L. M. Loew, Electric field-directed fibroblast locomotion involves cell surface molecular reorganization and is calcium independent. *The Journal of cell biology* 1994, 127. 117-28; (f) S. McLaughlin, M. M. Poo, The role of electro-osmosis in the electric-field-induced movement of charged macromolecules on the surfaces of cells. *Biophysical journal* 1981, 34. 85-93, DOI: 10.1016/s0006-3495(81)84838-2; (g) J. Han, X. L. Yan, Q. H. Han, Y. Li, J. Zhu, Y. N. Hui, Electric fields contribute to directed migration of human retinal pigment epithelial cells via interaction between F-actin and beta1 integrin. *Current eye research* 2009, 34. 438-46; (h) L. F. Jaffe, Electrophoresis along cell membranes. *Nature* 1977, 265. 600-2; (i) M. Poo, K. R. Robinson, Electrophoresis of concanavalin A receptors along embryonic muscle cell membrane. *Nature* 1977, 265. 602-5; (j) N. Orida, M. M. Poo, Electrophoretic movement and localisation of acetylcholine receptors in the embryonic muscle cell membrane. *Nature* 1978, 275. 31-5; (k) M. A. McCloskey, Z. Y. Liu, M. M. Poo, Lateral electromigration and diffusion of Fc epsilon receptors on rat basophilic leukemia cells: effects of IgE binding. *The Journal of cell biology* 1984, 99. 778-87.
19. F. X. Hart, M. Laird, A. Riding, C. Pullar, Keratinocyte galvanotaxis in combined DC and AC electric fields supports an electromechanical transduction sensing mechanism. *Bioelectromagnetics* 2013, 38.
20. (a) M. Zhao, B. Song, J. Pu, T. Wada, B. Reid, G. Tai, F. Wang, A. Guo, P. Walczysko, Y. Gu, T. Sasaki, A. Suzuki, J. V. Forrester, H. R. Bourne, P. N. Devreotes, C. D. McCaig, J. M. Penninger, Electrical signals control wound healing through phosphatidylinositol-3-OH kinase-gamma and PTEN. *Nature* 2006, 442. 457-60, DOI: 10.1038/nature04925; (b) J. Pu, M. Zhao, Golgi polarization in a strong electric field. *J Cell Sci* 2005, 118. 1117-28, DOI: 10.1242/jcs.01646; (c) X. Meng, M. Arocena, J. Penninger, F. H. Gage, M. Zhao, B. Song, PI3K mediated electrotaxis of embryonic and adult neural progenitor cells in the presence of growth factors. *Exp Neurol* 2011, 227. 210-7, DOI: 10.1016/j.expneurol.2010.11.002.
21. (a) A. J. Singer, R. A. Clark, Cutaneous wound healing. *The New England journal of medicine* 1999, 341. 738-46, DOI: 10.1056/nejm199909023411006; (b) E. T. Wang, M. Zhao, Regulation of tissue repair and regeneration by electric fields. *Chinese journal of traumatology = Zhonghua chuang shang za zhi / Chinese Medical Association* 2010, 13. 55-61; (c) P. Martin, Wound healing--aiming for perfect skin regeneration. *Science (New York, N.Y.)* 1997, 276. 75-81; (d) G. C. Gurtner, S. Werner, Y. Barrandon, M. T. Longaker, Wound repair and regeneration. *Nature* 2008, 453. 314-21, DOI: 10.1038/nature07039; (e) G. Fenteany, P. A. Janmey, T. P. Stossel, Signaling pathways and cell mechanics involved in wound closure by epithelial cell sheets. *Current biology : CB* 2000, 10. 831-8.
22. (a) Y. Jiang, B. N. Jahagirdar, R. L. Reinhardt, R. E. Schwartz, C. D. Keene, X. R. Ortiz-Gonzalez, M. Reyes, T. Lenvik, T. Lund, M. Blackstad, J. Du, S. Aldrich, A. Lisberg, W. C. Low, D. A. Largaespada, C. M. Verfaillie, Pluripotency of mesenchymal stem cells derived from adult marrow. *Nature* 2002, 418. 41-9, DOI: 10.1038/nature00870; (b) A. I. Caplan, Adult mesenchymal stem cells for tissue engineering versus regenerative medicine. *J Cell Physiol* 2007, 213. 341-7, DOI: 10.1002/jcp.21200; (c) M. F. Pittenger, A. M. Mackay, S. C. Beck, R. K. Jaiswal, R. Douglas, J. D. Mosca, M. A. Moorman, D. W. Simonetti, S. Craig, D. R. Marshak, Multilineage potential of adult human mesenchymal stem cells. *Science (New York, N.Y.)* 1999, 284. 143-7.
23. R. Secunda, R. Vennila, A. M. Mohanashankar, M. Rajasundari, S. Jeswanth, R. Surendran, Isolation, expansion and characterisation of mesenchymal stem cells from human bone marrow, adipose tissue, umbilical cord blood and matrix: a comparative study. *Cytotechnology* 2014. DOI: 10.1007/s10616-014-9718-z.
24. (a) C. A. Vacanti, L. J. Bonassar, M. P. Vacanti, J. Shufflebarger, Replacement of an avulsed phalanx with tissue-engineered bone. *The New England journal of medicine* 2001, 344. 1511-4, DOI: 10.1056/nejm200105173442004; (b) R. Quarto, M. Mastrogiacomo, R. Cancedda, S. M. Kutepov, V. Mukhachev, A. Lavroukov, E. Kon, M. Marcacci, Repair of large bone defects with the use of autologous bone marrow stromal cells. *The New*

- England journal of medicine* 2001, 344. 385-6, DOI: 10.1056/nejm200102013440516; (c) T. Morishita, K. Honoki, H. Ohgushi, N. Kotobuki, A. Matsushima, Y. Takakura, Tissue engineering approach to the treatment of bone tumors: three cases of cultured bone grafts derived from patients' mesenchymal stem cells. *Artificial organs* 2006, 30. 115-8, DOI: 10.1111/j.1525-1594.2006.00190.x; (d) H. Hibi, Y. Yamada, M. Ueda, Y. Endo, Alveolar cleft osteoplasty using tissue-engineered osteogenic material. *International journal of oral and maxillofacial surgery* 2006, 35. 551-5, DOI: 10.1016/j.ijom.2005.12.007; (e) H. Hibi, Y. Yamada, H. Kagami, M. Ueda, Distraction osteogenesis assisted by tissue engineering in an irradiated mandible: a case report. *The International journal of oral & maxillofacial implants* 2006, 21. 141-7; (f) H. Kitoh, T. Kitakoji, H. Tsuchiya, H. Mitsuyama, H. Nakamura, M. Katoh, N. Ishiguro, Transplantation of marrow-derived mesenchymal stem cells and platelet-rich plasma during distraction osteogenesis--a preliminary result of three cases. *Bone* 2004, 35. 892-8, DOI: 10.1016/j.bone.2004.06.013; (g) H. Kitoh, T. Kitakoji, H. Tsuchiya, M. Katoh, N. Ishiguro, Transplantation of culture expanded bone marrow cells and platelet rich plasma in distraction osteogenesis of the long bones. *Bone* 2007, 40. 522-8, DOI: 10.1016/j.bone.2006.09.019; (h) H. Kitoh, T. Kitakoji, H. Tsuchiya, M. Katoh, N. Ishiguro, Distraction osteogenesis of the lower extremity in patients with achondroplasia/hypochondroplasia treated with transplantation of culture-expanded bone marrow cells and platelet-rich plasma. *Journal of pediatric orthopedics* 2007, 27. 629-34, DOI: 10.1097/BPO.0b013e318093f523; (i) P. H. Warnke, I. N. Springer, J. Wiltfang, Y. Acil, H. Eufinger, M. Wehmoller, P. A. Russo, H. Bolte, E. Sherry, E. Behrens, H. Terheyden, Growth and transplantation of a custom vascularised bone graft in a man. *Lancet* 2004, 364. 766-70, DOI: 10.1016/s0140-6736(04)16935-3; (j) H. Ohgushi, N. Kotobuki, H. Funaoka, H. Machida, M. Hirose, Y. Tanaka, Y. Takakura, Tissue engineered ceramic artificial joint--ex vivo osteogenic differentiation of patient mesenchymal cells on total ankle joints for treatment of osteoarthritis. *Biomaterials* 2005, 26. 4654-61, DOI: 10.1016/j.biomaterials.2004.11.055; (k) K. Kawate, H. Yajima, H. Ohgushi, N. Kotobuki, K. Sugimoto, T. Ohmura, Y. Kobata, K. Shigematsu, K. Kawamura, K. Tamai, Y. Takakura, Tissue-engineered approach for the treatment of steroid-induced osteonecrosis of the femoral head: transplantation of autologous mesenchymal stem cells cultured with beta-tricalcium phosphate ceramics and free vascularized fibula. *Artificial organs* 2006, 30. 960-2, DOI: 10.1111/j.1525-1594.2006.00333.x.
25. (a) K. Gopal, H. A. Amirhamed, T. Kamarul, Advances of human bone marrow-derived mesenchymal stem cells in the treatment of cartilage defects: A systematic review. *Experimental biology and medicine (Maywood, N.J.)* 2014. DOI: 10.1177/1535370214530364; (b) A. Gobbi, G. Karnatzikos, S. R. Sankineani, One-step surgery with multipotent stem cells for the treatment of large full-thickness chondral defects of the knee. *The American journal of sports medicine* 2014, 42. 648-57, DOI: 10.1177/0363546513518007; (c) K. L. Wong, K. B. Lee, B. C. Tai, P. Law, E. H. Lee, J. H. Hui, Injectable cultured bone marrow-derived mesenchymal stem cells in varus knees with cartilage defects undergoing high tibial osteotomy: a prospective, randomized controlled clinical trial with 2 years' follow-up. *Arthroscopy : the journal of arthroscopic & related surgery : official publication of the Arthroscopy Association of North America and the International Arthroscopy Association* 2013, 29. 2020-8, DOI: 10.1016/j.arthro.2013.09.074.
26. (a) J. Zhang, M. Calafiore, Q. Zeng, X. Zhang, Y. Huang, R. A. Li, W. Deng, M. Zhao, Electrically guiding migration of human induced pluripotent stem cells. *Stem Cell Rev* 2011, 7. 987-96, DOI: 10.1007/s12015-011-9247-5; (b) J. F. Feng, J. Liu, X. Z. Zhang, L. Zhang, J. Y. Jiang, J. Nolta, M. Zhao, Guided migration of neural stem cells derived from human embryonic stem cells by an electric field. *Stem cells (Dayton, Ohio)* 2012, 30. 349-55, DOI: 10.1002/stem.779.
27. Z. Zhao, C. Watt, A. Karystinou, A. J. Roelofs, C. D. McCaig, I. R. Gibson, C. De Bari, Directed migration of human bone marrow mesenchymal stem cells in a physiological direct current electric field. *European cells & materials* 2011, 22. 344-58.
28. N. Tandon, B. Goh, A. Marsano, P. H. Chao, C. Montouri-Sorrentino, J. Gimble, G. Vunjak-Novakovic, Alignment and elongation of human adipose-derived stem cells in response to direct-current electrical stimulation. *Conf Proc IEEE Eng Med Biol Soc* 2009, 2009. 6517-21, DOI: 10.1109/iembs.2009.5333142.

29. K. E. Hammerick, M. T. Longaker, F. B. Prinz, In vitro effects of direct current electric fields on adipose-derived stromal cells. *Biochemical and biophysical research communications* 2010, **397**. 12-7, DOI: 10.1016/j.bbrc.2010.05.003.
30. Z. Wang, C. C. Clark, C. T. Brighton, Up-regulation of bone morphogenetic proteins in cultured murine bone cells with use of specific electric fields. *The Journal of bone and joint surgery. American volume* 2006, **88**. 1053-65, DOI: 10.2106/jbjs.e.00443.
31. H. Zhuang, W. Wang, R. M. Seldes, A. D. Tahernia, H. Fan, C. T. Brighton, Electrical stimulation induces the level of TGF-beta1 mRNA in osteoblastic cells by a mechanism involving calcium/calmodulin pathway. *Biochemical and biophysical research communications* 1997, **237**. 225-9, DOI: 10.1006/bbrc.1997.7118.
32. (a) C. T. Brighton, W. Wang, C. C. Clark, Up-regulation of matrix in bovine articular cartilage explants by electric fields. *Biochemical and biophysical research communications* 2006, **342**. 556-61, DOI: 10.1016/j.bbrc.2006.01.171; (b) W. Wang, Z. Wang, G. Zhang, C. C. Clark, C. T. Brighton, Up-regulation of chondrocyte matrix genes and products by electric fields. *Clinical orthopaedics and related research* 2004. S163-73.
33. P. F. Armstrong, C. T. Brighton, A. M. Star, Capacitively coupled electrical stimulation of bovine growth plate chondrocytes grown in pellet form. *Journal of orthopaedic research : official publication of the Orthopaedic Research Society* 1988, **6**. 265-71, DOI: 10.1002/jor.1100060214.
34. R. Hess, A. Jaeschke, H. Neubert, V. Hintze, S. Moeller, M. Schnabelrauch, H. P. Wiesmann, D. A. Hart, D. Scharnweber, Synergistic effect of defined artificial extracellular matrices and pulsed electric fields on osteogenic differentiation of human MSCs. *Biomaterials* 2012, **33**. 8975-85, DOI: 10.1016/j.biomaterials.2012.08.056.
35. (a) F. Luo, T. Hou, Z. Zhang, Z. Xie, X. Wu, J. Xu, Effects of pulsed electromagnetic field frequencies on the osteogenic differentiation of human mesenchymal stem cells. *Orthopedics* 2012, **35**. e526-31, DOI: 10.3928/01477447-20120327-11; (b) M. T. Tsai, W. J. Li, R. S. Tuan, W. H. Chang, Modulation of osteogenesis in human mesenchymal stem cells by specific pulsed electromagnetic field stimulation. *Journal of orthopaedic research : official publication of the Orthopaedic Research Society* 2009, **27**. 1169-74, DOI: 10.1002/jor.20862.
36. (a) M. Hronik-Tupaj, W. L. Rice, M. Cronin-Golomb, D. L. Kaplan, I. Georgakoudi, Osteoblastic differentiation and stress response of human mesenchymal stem cells exposed to alternating current electric fields. *Biomedical engineering online* 2011, **10**. 9, DOI: 10.1186/1475-925x-10-9; (b) C. M. Creecy, C. F. O'Neill, B. P. Arulanandam, V. L. Sylvia, C. S. Navara, R. Bizios, Mesenchymal stem cell osteodifferentiation in response to alternating electric current. *Tissue engineering. Part A* 2013, **19**. 467-74, DOI: 10.1089/ten.TEA.2012.0091.
37. S. D. McCullen, J. P. McQuilling, R. M. Grossfeld, J. L. Lubischer, L. I. Clarke, E. G. Lobo, Application of low-frequency alternating current electric fields via interdigitated electrodes: effects on cellular viability, cytoplasmic calcium, and osteogenic differentiation of human adipose-derived stem cells. *Tissue engineering. Part C, Methods* 2010, **16**. 1377-86, DOI: 10.1089/ten.TEC.2009.0751.
38. E. Esfandiari, S. Roshankhah, M. Mardani, B. Hashemibeni, E. Naghsh, M. Kazemi, M. Salahshoor, The effect of high frequency electric field on enhancement of chondrogenesis in human adipose-derived stem cells. *Iranian journal of basic medical sciences* 2014, **17**. 571-6.
39. K. E. Hammerick, A. W. James, Z. Huang, F. B. Prinz, M. T. Longaker, Pulsed direct current electric fields enhance osteogenesis in adipose-derived stromal cells. *Tissue engineering. Part A* 2010, **16**. 917-31, DOI: 10.1089/ten.TEA.2009.0267.
40. M. A. Matos, M. T. Cicerone, Alternating current electric field effects on neural stem cell viability and differentiation. *Biotechnology progress* 2010, **26**. 664-70, DOI: 10.1002/btpr.389.
41. H. Cui, L. Tang, Stem cell lineage commitment by electrical fields and the potential application in drug discovery. *Current drug metabolism* 2013, **14**. 272-8.
42. (a) USA, 2010; (b) S. Gronthos, S. Fitter, P. Diamond, P. J. Simmons, S. Itescu, A. C. Zannettino, A novel monoclonal antibody (STRO-3) identifies an isoform of tissue nonspecific alkaline phosphatase expressed by multipotent bone marrow stromal stem cells. *Stem cells and development* 2007, **16**. 953-63, DOI: 10.1089/scd.2007.0069.
43. E. Finkelstein, W. Chang, P. H. Chao, D. Gruber, A. Minden, C. T. Hung, J. C. Bulinski, Roles of microtubules, cell polarity and adhesion in electric-

- field-mediated motility of 3T3 fibroblasts. *Journal of cell science* 2004, **117**. 1533-45, DOI: 10.1242/jcs.00986.
44. M. Zhao, H. Bai, E. Wang, J. V. Forrester, C. D. McCaig, Electrical stimulation directly induces pre-angiogenic responses in vascular endothelial cells by signaling through VEGF receptors. *Journal of cell science* 2004, **117**. 397-405, DOI: 10.1242/jcs.00868.
45. Y. Huang, J. Samorajski, R. Kreimer, P. Searson, The influence of electric field and confinement on cell motility. *PLoS ONE* 2013, **8**. e59447.
46. Y. Huang, X.-B. Wang, F. F. Becker, P. Gascoyne, Introducing dielectrophoresis as a new force field for field-flow fractionation. *Biophysical journal* 1997, **73**. 1118-1129.
47. A. Szymczyk, Y. I. Dirir, M. Picot, I. Nicolas, F. Barriere, Advanced electrokinetic characterization of composite porous membranes. *Journal of Membrane Science* 2013, **429**. 44-51, DOI: 10.1016/j.memsci.2012.11.076.
48. T. Glawdel, C. L. Ren, Electro-osmotic flow control for living cell analysis in microfluidic PDMS chips. *Mechanics Research Communications* 2009, **36**. 75-81, DOI: <http://dx.doi.org/10.1016/j.mechrescom.2008.06.015>.
49. A. E. Carpenter, T. R. Jones, M. R. Lamprecht, C. Clarke, I. H. Kang, O. Friman, D. A. Guertin, J. H. Chang, R. A. Lindquist, J. Moffat, P. Golland, D. M. Sabatini, CellProfiler: image analysis software for identifying and quantifying cell phenotypes. *Genome biology* 2006, **7**. R100, DOI: 10.1186/gb-2006-7-10-r100.
50. A. T. Barker, L. F. Jaffe, J. W. Vanable, Jr., The glabrous epidermis of cavies contains a powerful battery. *Am J Physiol* 1982, **242**. R358-66.
51. P. C. Chang, G. I. Sulik, H. K. Soong, W. C. Parkinson, Galvanotropic and galvanotaxic responses of corneal endothelial cells. *J Formos Med Assoc* 1996, **95**. 623-7.
52. C. W. Huang, J. Y. Cheng, M. H. Yen, T. H. Young, Electrotaxis of lung cancer cells in a multiple-electric-field chip. *Biosens Bioelectron* 2009, **24**. 3510-6, DOI: 10.1016/j.bios.2009.05.001.
53. (a) X. Li, J. Kolega, Effects of direct current electric fields on cell migration and actin filament distribution in bovine vascular endothelial cells. *Journal of vascular research* 2002, **39**. 391-404, DOI: 64517; (b) N. Ozkucur, T. K. Monsees, S. Perike, H. Q. Do, R. H. Funk, Local calcium elevation and cell elongation initiate guided motility in electrically stimulated osteoblast-like cells. *PLoS one* 2009, **4**. e6131, DOI: 10.1371/journal.pone.0006131; (c) Z. Zhao, L. Qin, B. Reid, J. Pu, T. Hara, M. Zhao, Directing migration of endothelial progenitor cells with applied DC electric fields. *Stem cell research* 2012, **8**. 38-48, DOI: 10.1016/j.scr.2011.08.001.
54. P. H. Chao, H. H. Lu, C. T. Hung, S. B. Nicoll, J. C. Bulinski, Effects of applied DC electric field on ligament fibroblast migration and wound healing. *Connect Tissue Res* 2007, **48**. 188-97, DOI: 10.1080/03008200701424451.
55. D. M. Sheridan, R. R. Isseroff, R. Nuccitelli, Imposition of a physiologic DC electric field alters the migratory response of human keratinocytes on extracellular matrix molecules. *J Invest Dermatol* 1996, **106**. 642-6.
56. E. K. Onuma, S. W. Hui, Electric field-directed cell shape changes, displacement, and cytoskeletal reorganization are calcium dependent. *J Cell Biol* 1988, **106**. 2067-75.
57. L. Li, W. Gu, J. Du, B. Reid, X. Deng, Z. Liu, Z. Zong, H. Wang, B. Yao, C. Yang, J. Yan, L. Zeng, L. Chalmers, M. Zhao, J. Jiang, Electric fields guide migration of epidermal stem cells and promote skin wound healing. *Wound repair and regeneration : official publication of the Wound Healing Society [and] the European Tissue Repair Society* 2012, **20**. 840-51, DOI: 10.1111/j.1524-475X.2012.00829.x.
58. (a) E. I. Finkelstein, P. H. Chao, C. T. Hung, J. C. Bulinski, Electric field-induced polarization of charged cell surface proteins does not determine the direction of galvanotaxis. *Cell motility and the cytoskeleton* 2007, **64**. 833-46, DOI: 10.1002/cm.20227; (b) B. Rapp, A. de Boisfleury-Chevance, H. Gruler, Galvanotaxis of human granulocytes. Dose-response curve. *Eur Biophys J* 1988, **16**. 313-9; (c) J. Li, S. Nandagopal, D. Wu, S. F. Romanuik, K. Paul, D. J. Thomson, F. Lin, Activated T lymphocytes migrate toward the cathode of DC electric fields in microfluidic devices. *Lab on a chip* 2011, **11**. 1298-304, DOI: 10.1039/c0lc00371a.
59. R. Babona-Pilipos, M. R. Popovic, C. M. Morshead, A galvanotaxis assay for analysis of neural precursor cell migration kinetics in an externally applied direct current electric field. *Journal of visualized experiments : JoVE* 2012. DOI: 10.3791/4193.

60. (a) C. A. Erickson, Nuccitelli, R., Embryonic fibroblast motility and orientation can be influenced by physiological electric fields. *J. Cell. Biol* 1984, *98*. 296–307; (b) M. S. Cooper, R. E. Keller, Perpendicular orientation and directional migration of amphibian neural crest cells in dc electrical fields. *Proceedings of the National Academy of Sciences of the United States of America* 1984, *81*. 160-4.
61. N. Tandon, C. Cannizzaro, P. H. Chao, R. Maidhof, A. Marsano, H. T. Au, M. Radisic, G. Vunjak-Novakovic, Electrical stimulation systems for cardiac tissue engineering. *Nat Protoc* 2009, *4*. 155-73, DOI: 10.1038/nprot.2008.183.
62. L. Cao, J. Pu, M. Zhao, GSK-3beta is essential for physiological electric field-directed Golgi polarization and optimal electrotaxis. *Cellular and molecular life sciences : CMLS* 2011, *68*. 3081-93, DOI: 10.1007/s00018-010-0608-z.
63. J. Zhang, R. Ren, X. Luo, P. Fan, X. Liu, S. Liang, L. Ma, P. Yu, H. Bai, A small physiological electric field mediated responses of extravillous trophoblasts derived from HTR8/SVneo cells: involvement of activation of focal adhesion kinase signaling. *PLoS One* 2014, *9*. e92252, DOI: 10.1371/journal.pone.0092252.
64. X. Yan, J. Han, Z. Zhang, J. Wang, Q. Cheng, K. Gao, Y. Ni, Y. Wang, Lung cancer A549 cells migrate directionally in DC electric fields with polarized and activated EGFRs. *Bioelectromagnetics* 2009, *30*. 29-35, DOI: 10.1002/bem.20436.
65. M. Zhao, J. Pu, J. V. Forrester, C. D. McCaig, Membrane lipids, EGF receptors, and intracellular signals colocalize and are polarized in epithelial cells moving directionally in a physiological electric field. *Faseb J* 2002, *16*. 857-9, DOI: 10.1096/fj.01-0811fje.
66. M. J. Sato, H. Kuwayama, W. N. van Egmond, A. L. Takayama, H. Takagi, P. J. van Haastert, T. Yanagida, M. Ueda, Switching direction in electric-signal-induced cell migration by cyclic guanosine monophosphate and phosphatidylinositol signaling. *Proceedings of the National Academy of Sciences of the United States of America* 2009, *106*. 6667-72, DOI: 10.1073/pnas.0809974106.
67. I. R. Nishimura KY, Nuccitelli R. , Human keratinocytes migrate to the negative pole in direct current electric fields comparable to those measured in mammalian wounds. *Journal of cell science* 1996, *109*. 199-207.
68. M. Poo, J. W. Lam, N. Orida, A. W. Chao, membrane. *Biophys J* 1979, *26*. 1-21, DOI: 10.1016/s0006-3495(79)85231-5.
69. M. Arocena, M. Zhao, J. M. Collinson, B. Song, A time-lapse and quantitative modelling analysis of neural stem cell motion in the absence of directional cues and in electric fields. *Journal of neuroscience research* 2010, *88*. 3267-74, DOI: 10.1002/jnr.22502.
70. H. Y. Yang, R. P. Charles, E. Hummler, D. L. Baines, R. R. Isseroff, The epithelial sodium channel mediates the directionality of galvanotaxis in human keratinocytes. *Journal of cell science* 2013, *126*. 1942-51, DOI: 10.1242/jcs.113225.
71. M. Zhao, L. Chalmers, L. Cao, A. C. Vieira, M. Mannis, B. Reid, Electrical signaling in control of ocular cell behaviors. *Progress in retinal and eye research* 2012, *31*. 65-88, DOI: 10.1016/j.preteyeres.2011.10.001.